Geophysical Research Letters

Supporting Information for

The influence of earthquake gates on surface rupture length

A.M. Rodriguez Padilla [1,2*], M.E. Oskin[1], E.E. Brodsky[3], K. Dascher-Cousineau[4], V. Herrera[5], S. White[6,7]

[1] Department of Earth and Planetary Sciences, University of California, Davis

[2] Now at Division of Geological and Planetary Sciences, California Institute of Technology

[3] Department of Earth and Planetary Sciences, University of California, Santa Cruz

[4] Department of Earth and Planetary Sciences, University of California, Berkeley

[5] Department of Earth and Environmental Sciences, San Diego State University

[6] Geology Department, Pasadena City College

[7]Now at Department of Earth, Planetary, and Space Sciences, University of California, Los Angeles

*Corresponding author: Alba M. Rodriguez Padilla (alba@caltech.edu, amrodriguezpadilla@gmail.com)

Contents of this file

Supplementary Methods

Figures S1 to S10

Table S11

Ks-test results and passing probabilities

Rupture termini documentation

Earthquake gate maps for each event

Introduction

This file contains the mapping method followed, supplementary figures S1 to S11, table S12, and the maps of each event and its corresponding earthquake gate. The maps are generated in 30 x 30 in files at 300 dpi so that they can be easily zoomed into and examined.

Supplementary Methods

Earthquake Gate Mapping

We choose to focus on strike-slip events because vertically dipping faults tend to remain constant in dip with depth so that surface geometry, besides fine-scale heterogeneity, can be used as a proxy for the geometry at depth. We rely on the surface rupture maps compiled in the Fault Displacement Hazard Initiative (FDHI) database (Sarmiento et al., 2021). At the time of access for this manuscript (May, 2022), the database encompassed sixty-six, globally distributed, surface rupturing earthquakes (M_w 5-8), of which thirty-one are strike-slip. The database includes surface rupture maps for each event, were ruptures are classified as primary or distributed, displacement measurements, and additional information, such as lithology or slope. Surface ruptures are mapped to 1-meter precision in the database, though individual maps differ in the level of detail captured in the surface rupture. This variability is in part related to the different degrees of complexity in the hosting fault system, and in part a result of differences in mapping methods and extent across ruptures.

We map earthquake gates from the surface ruptures in the FDHI database at a 1:50,000 scale, which roughly corresponds to mapping features with lengths exceeding 100-500 meters. At this scale, we expect the level of detail across ruptures to be roughly comparable. The surface rupture maps in the FDHI database include ruptures classified as principal and distributed. To ensure that we only include primary faults, which are the seismogenic structures in the events in our analysis, we consider the ruptures characterized as principal in the database. This also allows for comparison across events with different spatial coverage of the off-fault deformation field.

Prior work has either relied on simplified rupture maps (e.g., Wesnousky, 2006) or simplified ruptures to segments long enough (~7 km) to make results commensurable with UCERF3 model discretization and comparable to standard fault maps (Biasi and Wesnousky, 2017, 2021). We map earthquake gates directly from the surface rupture maps, without simplifying the rupture traces. An important consequence of our scale of choice (1:50,000) is that larger features (for example, the large, regional-scale releasing bend in the Balochistan earthquake which spans 6 km) are mapped into its smaller constituents that occur at the mapping scale (i.e. several shorter bends that make up the regional one). Our scale of choice results in the mapping of smaller step-overs that were previously not classified in prior work due to their small size but does not influence the maximum breached step-over width that can be measured as long as the step is not hard-linked, in which case it would be mapped as a bend or a splay.

We characterize gates as restraining or releasing when possible, depending on the volumetric deformation fostered by the type of slip and the geometry of the fault segments. To do this, we assume all fault segments involved in the rupture have strike-slip kinematics consistent with the focal mechanism for the event. At large scales, this is a reasonable approximation for all the strike-slip ruptures in the FDHI database except for the Denali earthquake, from which we remove the portion of the rupture that occurred on the Susitna Glacier Thrust, where the earthquake initiated (e.g., Crone et al., 2004). However, at finer scales, including our mapping scale, transitions from strike-slip to more oblique or vertical slip can lead to larger bend angles. We do not account for this limitation due to the absence of information to do so consistently for all events, following the rationale of Biasi and Wesnousky (2017).

A portion of the Kobe earthquake ruptured offshore and is not available in our map, with the section being onshore also being only a partial rupture to the surface, resulting in comparatively short surface rupture for the event magnitude. Incomplete rupture to the surface is also a limitation that applies to the smaller magnitude events considered here, such as the Chalfant Valley earthquake.

We characterize five different types of earthquake gates in this study: step-overs, gaps, bends, splays, and strands (Figure 1). We distinguish between breached features where the rupture transferred through and continued for at least 1 kilometer, and unbreached features, where the rupture halted immediately or within 1 km past the gate. For the case of splays, we classify cases where the rupture transferred onto a splay (regardless of whether it also continued on the main fault), as ruptured and instances where an available intersecting splay fault was foregone as unruptured. Note the use of different terminology from breached and unbreached to indicate that at least one fault strand was always active past the splay (Figure 1).

For each of the gates of interest, we measure the relevant geometrical attribute. For bends and splays, this is the bend angle, which is the difference between the fault strike as it enters the feature and the fault strike as it exits the feature. In the case of multi-stranded bends, we map the bend strand with the smallest angle. We distinguish between single bends, where the fault strike changes once, and double bends, where the fault strike changes for a segment and then returns to the original strike (see examples in Figure 1). Because natural double bends have angles that are not perfectly identical on each side of the bend limb, we take the average of the two angles. In most cases, the angle difference between the two angles is well below 10 degrees. Step-overs occur where a fault ends and the rupture is forced to jump onto a neighboring segment or come to arrest. We also map locations where the rupture activates parallel to subparallel neighboring fault strands without reaching the terminus of the principal fault. By definition, strands may only exist as breached features, as there was no fault terminus that forced a jump. For step-overs and strands, we measure the distance between parallel or subparallel fault segments at their minimum, orthogonal to the fault segments when possible. For gaps, we measure the length of the gap between the active rupture and another fault, or between parts of the active rupture if breached, in the fault-parallel direction. Note that we do not have the ability to distinguish gaps that represent pauses on the rupture on the same fault versus gaps that represent the spacing between two sequential faults of parallel strike.

We rely on different active fault databases to characterize unbreached features, where we measure the angle or distance between the ruptured fault and unruptured active faults in the database. The reference databases we use are listed in Supplementary Table S11. For the United States, the resolution of the regional faults associated with the events in this study in the Qfaults database is comparable to the resolution of the primary rupturing faults in the FDHI database. For the Darfield event in New Zealand, we use the NZAFD database, mapped at 1:250,000 (Langridge et al., 2016). The Active Faults of Eurasia Database (AFEAD) database for Eurasia, which we use for events in Turkey and Asia, is mapped at 1:500,000 scale (Bachmanov et al., 2021). Last, the GEM database, which we use only for the San Miguel and Pisayambo earthquakes in Mexico and Ecuador respectively, is mapped at 1:1,000,000 scale (Styron and Pagani, 2020). In the interest of classifying unbreached features as restraining or releasing, when the inactive fault kinematics are unknown, we assume these are the same as the rupturing faults'. When two unbreached step-overs may be measured at a fault's terminus, we map both, following the choice of previous workers (e.g., Wesnousky, 2006). Note that some events (e.g., Galway Lake and Ridgecrest foreshock) have unbreached step-overs at both of their termini with the same fault (e.g., the faults in the Landers event and the Garlock fault respectively), in which case both unbreached step-overs are mapped. When a gap and a step-over of the same size exist, and one gets breached but the other one does not, we map both the breached and unbreached features. The same occurs where there is a bend but the rupture instead skips the bend and jumps ahead to a more straight portion of the fault. This only occurs in the case of very similarly sized earthquake gates available at the same location, otherwise, we only map the smallest gate present. We provide our mapped earthquake gates as shapefiles (see data availability section) and shown over the rupture maps and regional fault maps in this supplementary section.

Passing Probability and Event Likelihood Estimates

To determine whether the forms of geometrical complexity we map (Figure 1) act as barriers to rupture propagation, we analyze the distribution of breached and unbreached gates in terms of the geometrical attribute measured (angle or length). We look at the cumulative distribution functions of breached and unbreached gates and use a Kolmogorov-Smirnoff (KS) test to determine whether the breached and unbreached populations are statistically different.

For those features where the breached and unbreached populations are statistically different (Figure 2), we compute passing probabilities as a function of the geometrical characteristics of the gate. To do so, we use a logistic function, which describes the probability of a binary outcome (breached or unbreached) as a continuous function of the geometry of an earthquake gate. To fit logistic regressions through our data, we use the Python package scikit learn (Pedregosa et al., 2011). An advantage of using logistic regressions over past methods is that estimating probabilities does not rely on arbitrary binning of the data. We evaluate the performance of our logistic models for each type of earthquake gate using Receiver Operating Characteristic (ROC) scores and confusion matrices, which is standard procedure for these models (Pedregosa et al., 2011). ROC scores can range from 0.5 to 1, with increasing values indicating that more data points have been correctly predicted by the logistic regression.

Supplementary Figures

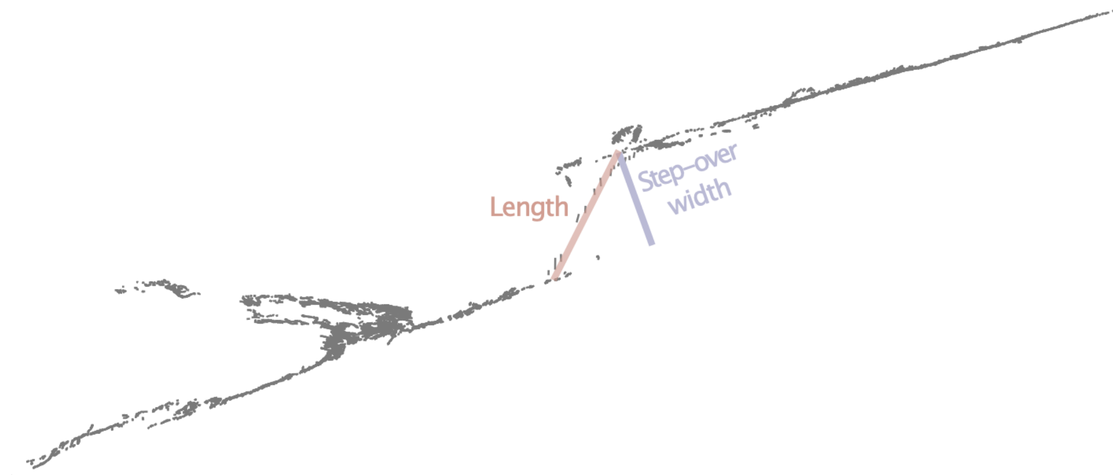

Figure S1. Releasing double bend from the 2014 Yutian earthquake. The rupture map is shown in gray. The pink and purple lines show the bend length as defined by Lozos et al. (2011) and the proxy step-over width respectively. The proxy step-over width is ~2.5 km wide.

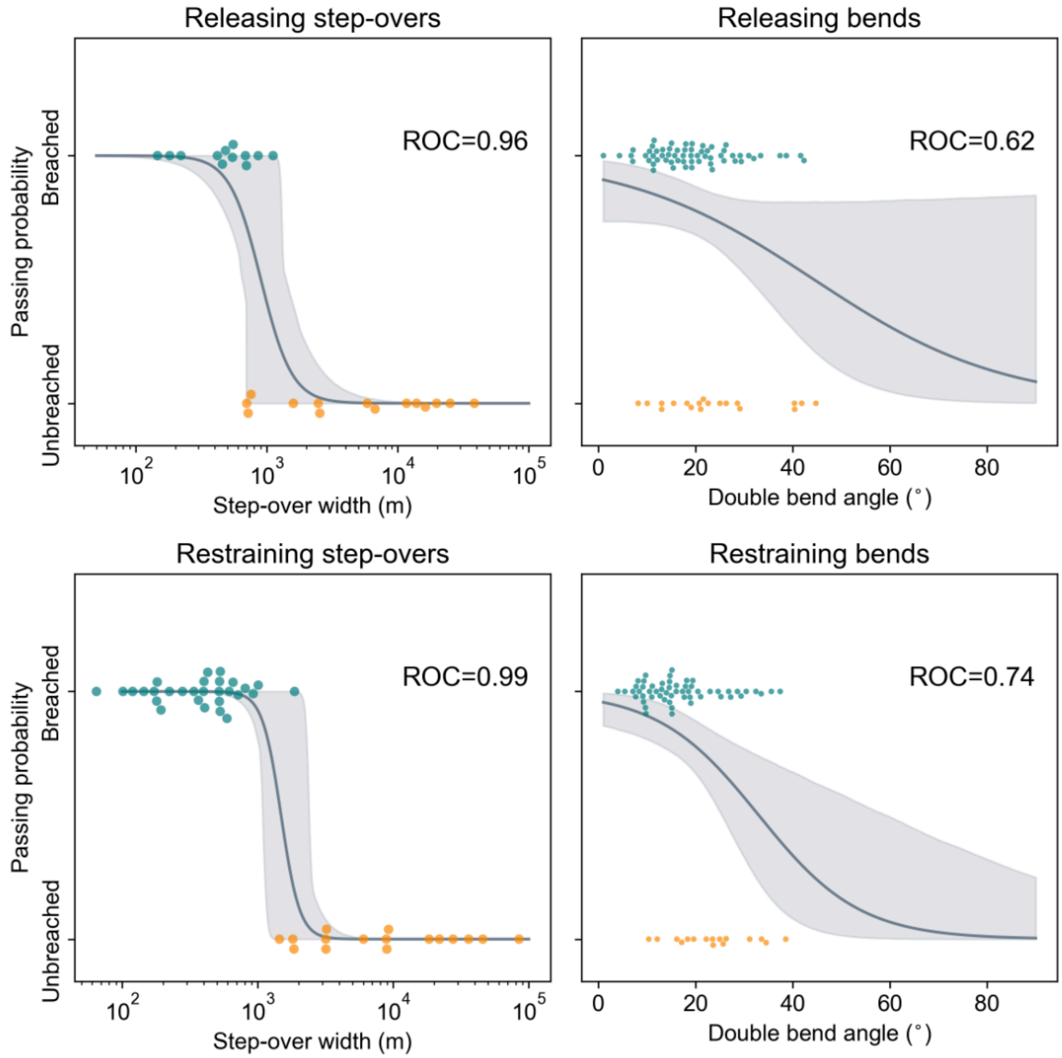

Figure S2. Logistic regressions (gray) showing the passing probabilities of restraining and releasing step-overs and double bends. The data are shown as beehive plots, which show all data points in each classification, breached in teal and unbreached in orange. The ROC score for each logistic regression is shown on the top right of each panel. Top and bottom left: Passing probability as a function of step-over width. Top and bottom right: Passing probability as a function of double bend angle. The gray shading shows the 95% confidence intervals of the regressions calculated by bootstrapping.

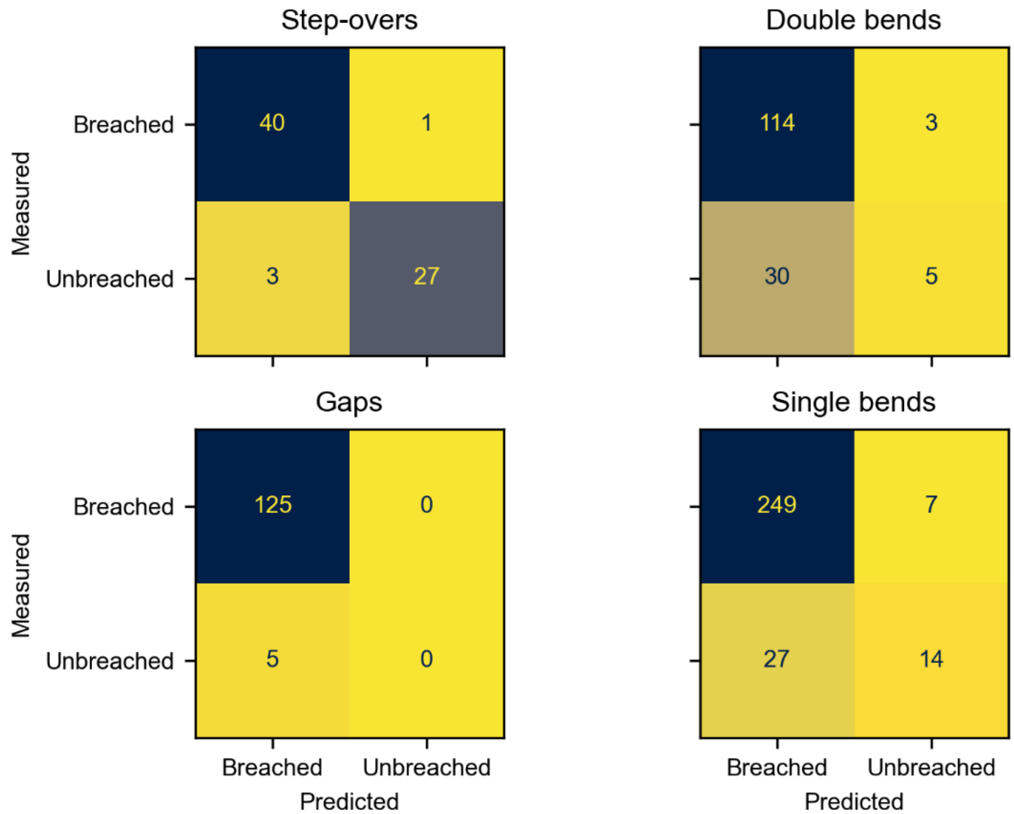

Figure S3. Confusion matrices for the logistic models for step-overs, single and double bends, and gaps in Figure 3. Darker colors in the matching diagonals indicate better diagnosis of the breached and unbreached features by the logistic fits.

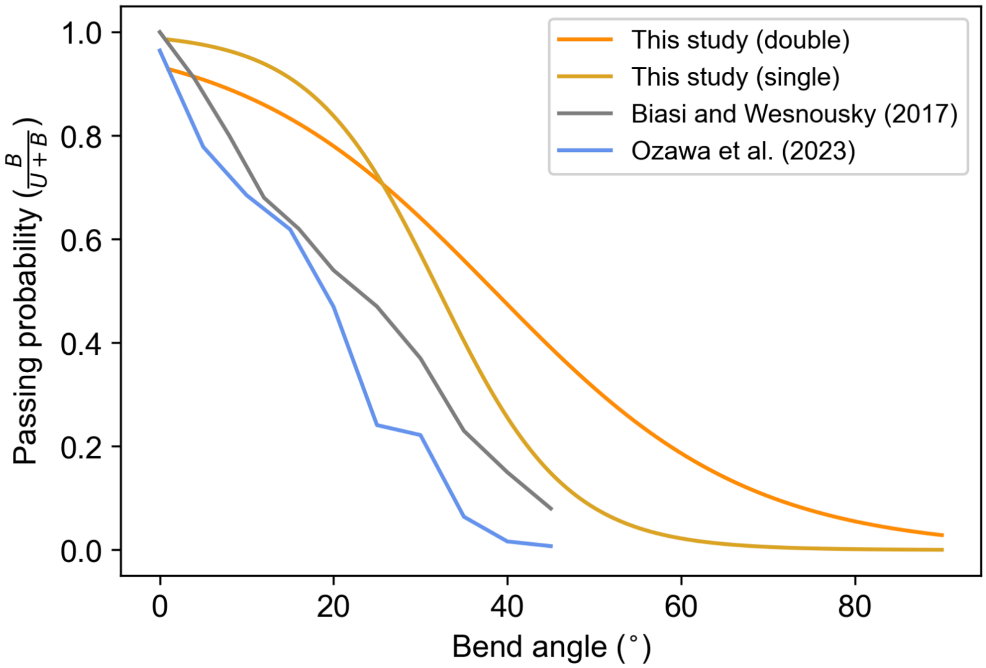

Figure S4. Comparison of the passing probabilities for different bend angles estimated in Biasi and Wesnousky (2017), Ozawa et al. (2023), and this study. Passing probability estimated as the number of breached bends per bin over the total number of bends in that bin in previous studies and with logistic regressions here. Note that the Biasi and Wesnousky (2017) passing probabilities include both single and double bends without discriminating between them, and the Ozawa et al. (2023) passing probabilities only include double bends.

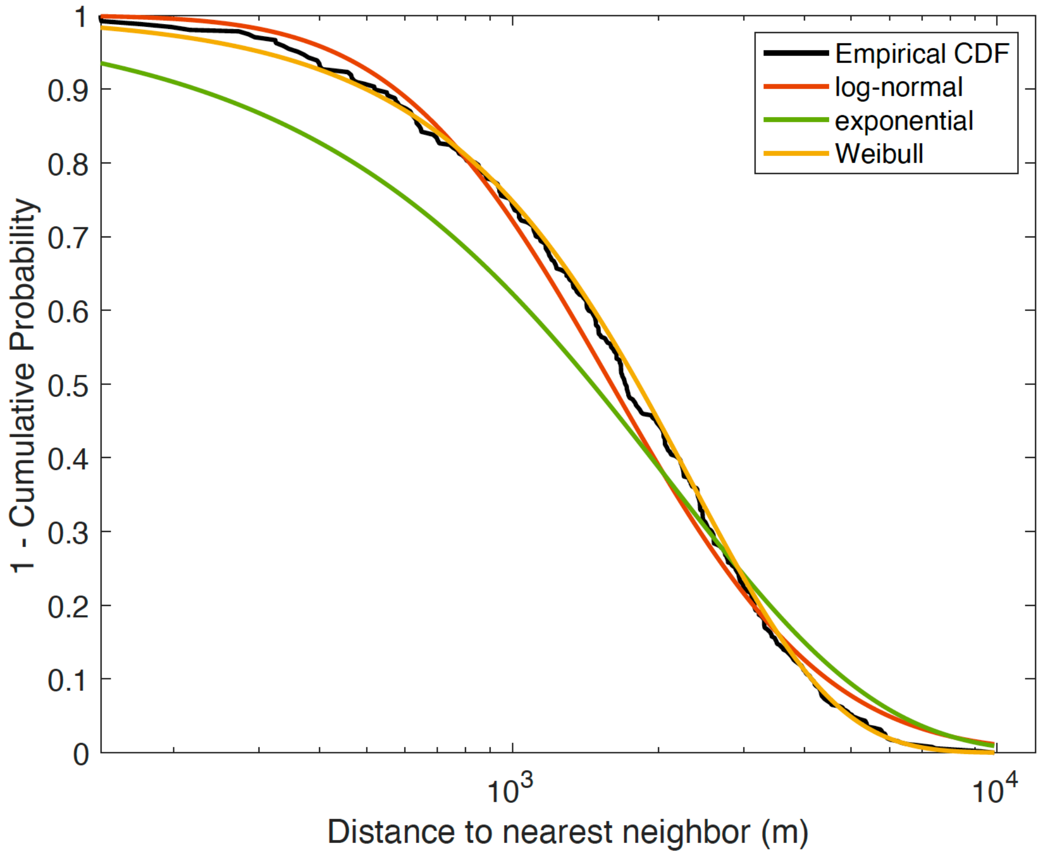

Figure S5. Empirical complementary cumulative distribution function of the distances to nearest neighbor for all breached earthquake gates. Complementary cumulative distribution functions for a log-normal, an exponential, and a Weibull fit are shown in orange, green, and yellow, respectively.

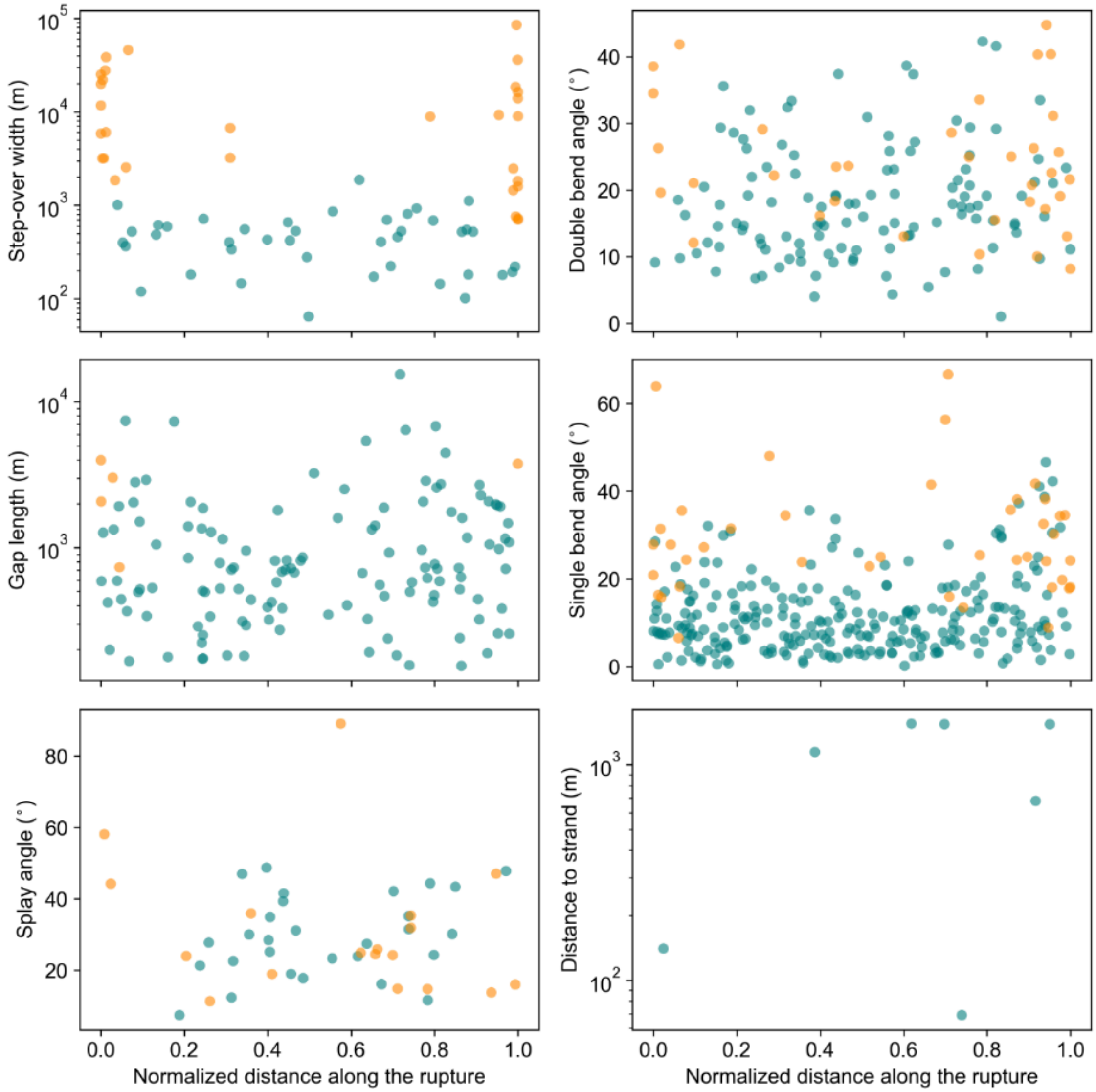

Figure S6. Distribution of breached (teal) and unbreached (orange) earthquake gates along the normalized surface rupture lengths of the 31 strike-slip events. The rupture lengths are based on the FDHI database event coordinate systems (ECS) reference lines (Sarmiento et al., 2021). There are some unbreached gates not at the edge of the ruptures. This is because, at some locations, there were two or more earthquake gates available, so that the gate the rupture continues past is mapped as breached and the remaining ones get mapped as unbreached (see methods for details).

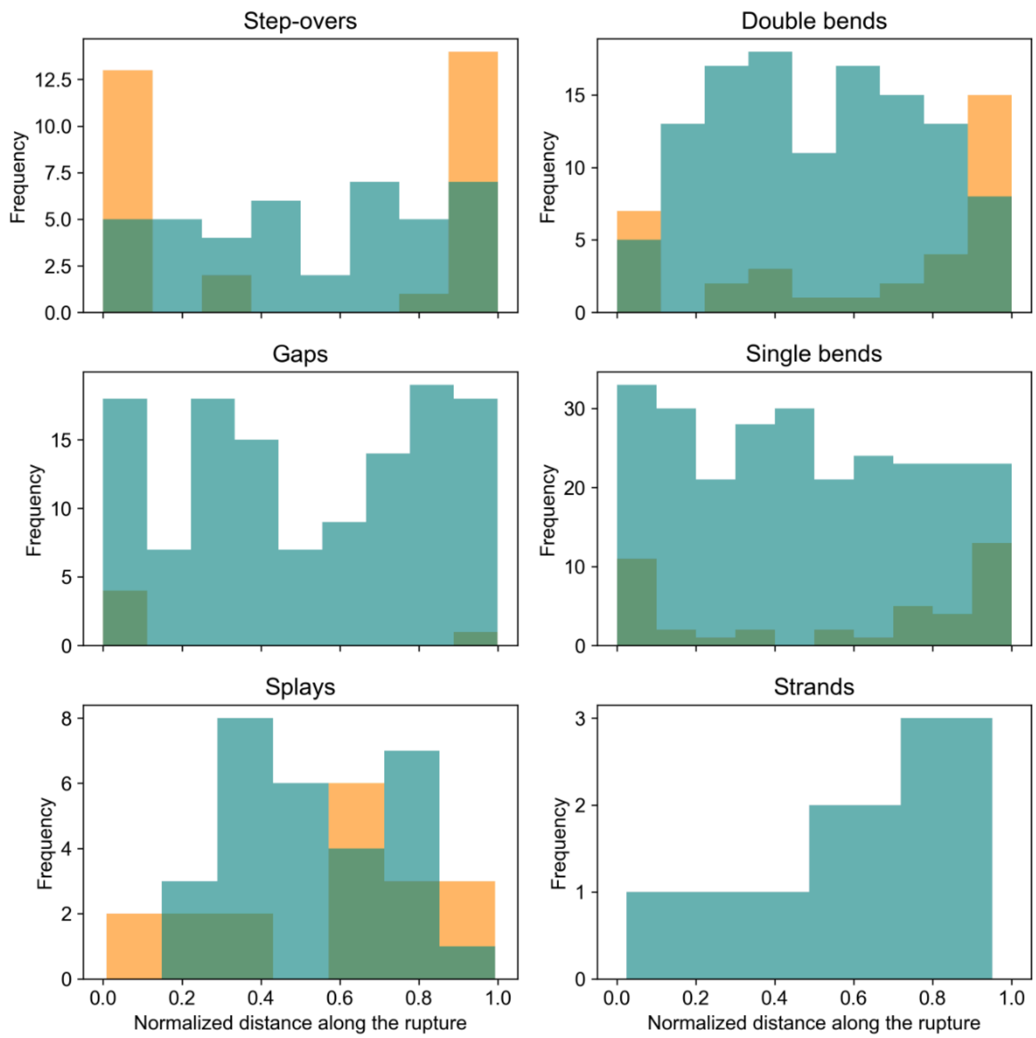

Figure S7. Frequency of earthquake gates, breached and unbreached in teal and orange respectively, along the normalized surface rupture length for each earthquake gate type. Transparency is used to allow for visualization of the unbreached boxes (orange). Because we do not consider rupture propagation direction, as it is unknown for many of the events, the orientation of the x axis of this plot does not carry meaning.

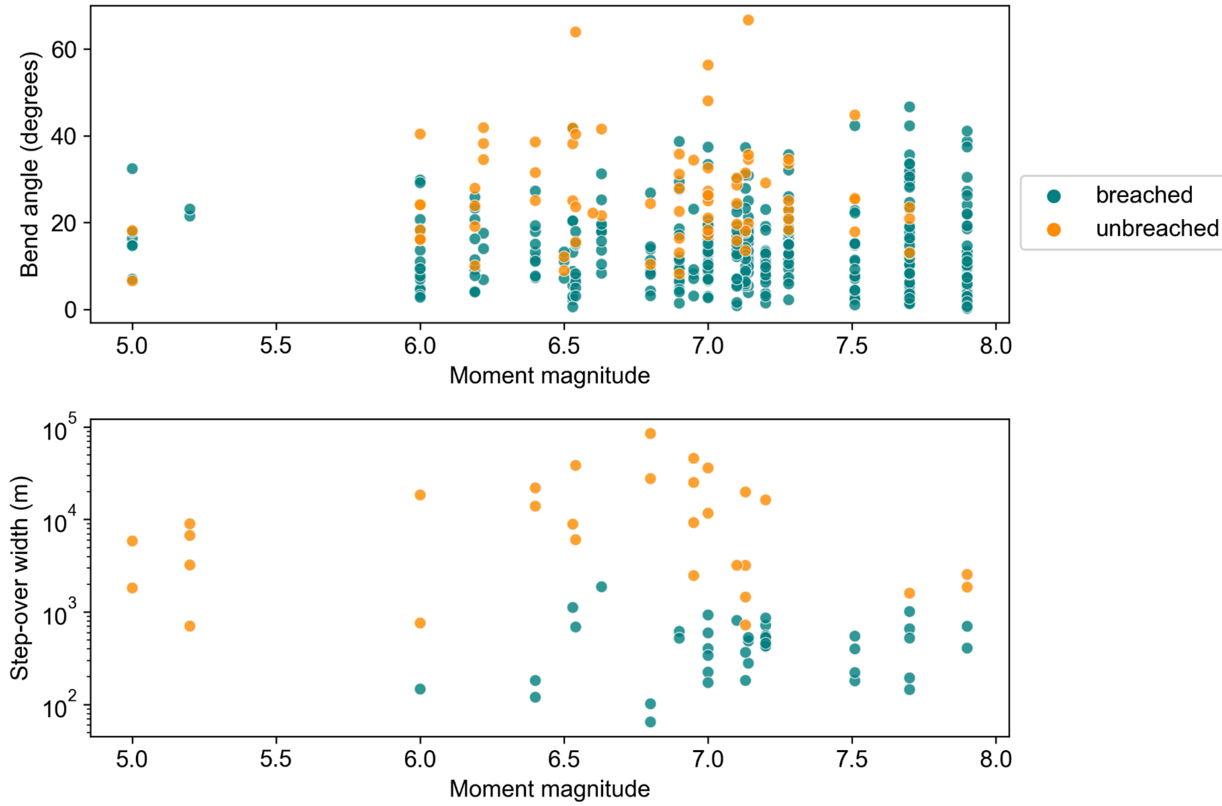

Figure S8. Bend angle (top) and step-over width (bottom) versus event moment magnitude for each of the events considered in this study.

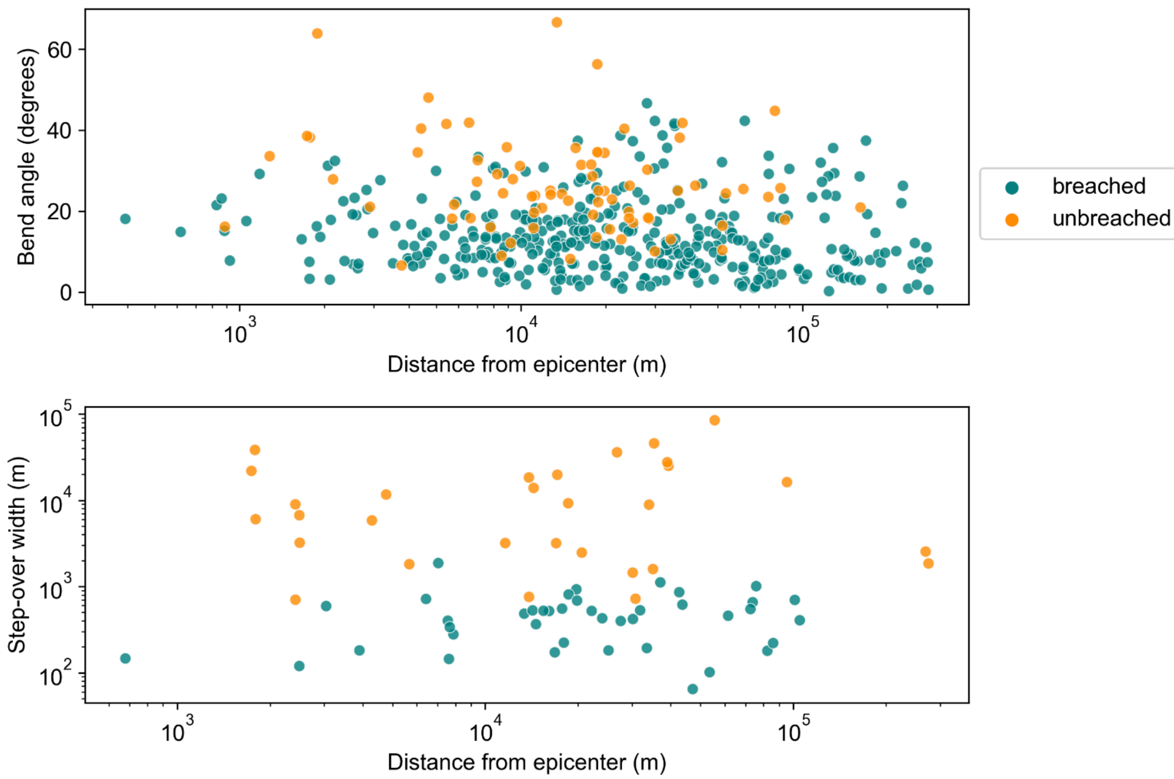

Figure S9. Gate size versus minimum distance to event epicenter. The event epicenters are sourced from the FDHI database (Sarmiento et al. (2021). Note some epicenters in the database are off-fault.

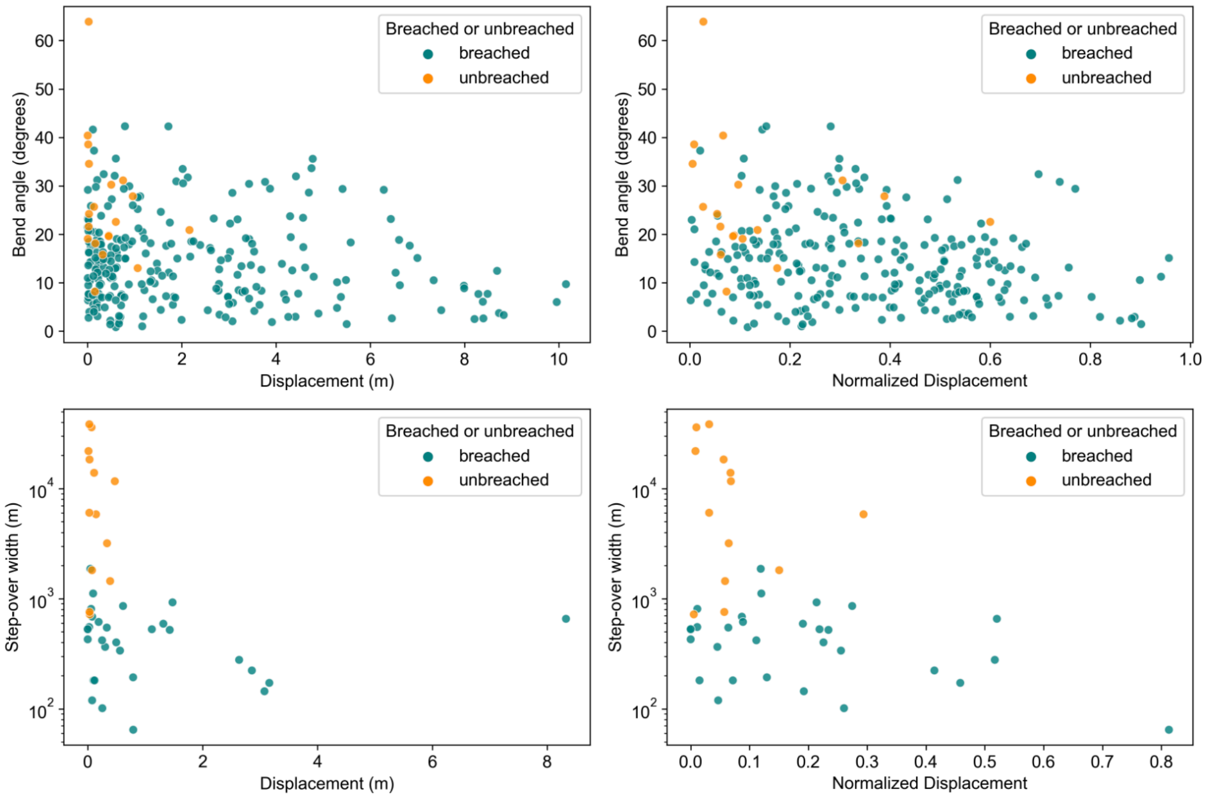

Figure S10. Average slip at bends (top), including both single and double bends, and step-overs (bottom) as a function of bend angle and step-over width. The slip is computed as the average value for all slip measurements available within 500 meters of the earthquake gate. The plots on the left have the mean slip and the ones on the right have the mean slip normalized by the maximum slip of the event the gate was measured for.

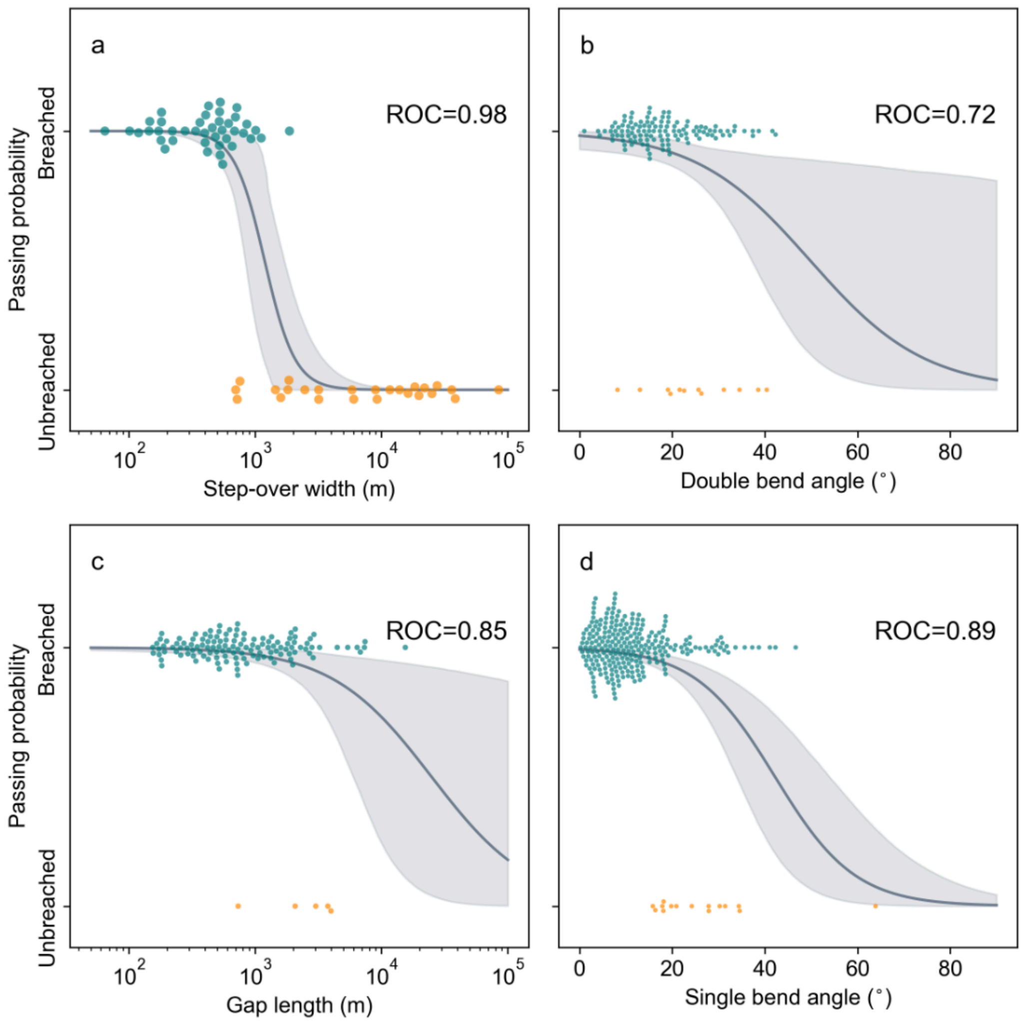

Figure S11. Passing probabilities as a function of geometry including only unbreached earthquake gates at rupture termini (within 5% of the rupture length of each termini). All breached gates are included.

Reference Fault Map	Location	References
Quaternary Fault and Fold Database of the United States	United States	USGS and CGS
New Zealand Active Faults Database (NZAFD)	New Zealand	Langridge et al. (2016)
The Active Faults of Eurasia Database (AFEAD)	Europe and Asia	Bachmanov et al. (2021)
GEM Global Active Faults Database	Central and South America	Styron and Pagani (2020)

Table S12. Reference maps of active faults to measure unbreached feature characteristics with respect to.

1 Number of mapped features

Feature	Number mapped
Step-overs	71
Releasing step-overs	26
Restraining step-overs	45
Bends	449
Single bends	297
Double bends	152
Releasing double bends	80
Restraining double bends	72
Gaps	130
Splays	47
Strands	7

2 p-values from the ks tests

Feature A	Feature B	p-value from ks test
Breached double bend	Unbreached double bend	5.049231e-03
Breached single bend	Unbreached single bend	2.679407e-17
Breached step-over	Unbreached step-over	2.340031e-14
Breached gaps	Unbreached gaps	1.418856e-02
Breached splay	Unbreached splay	6.938317e-01
Releasing unbreached bend	Restraining unbreached bend	7.370006e-01
Releasing breached bend	Restraining breached bend	1.402596e-01
Releasing breached step-over	Restraining breached step-over	4.827584e-01
Releasing unbreached step-over	Restraining unbreached step-over	6.820546e-01

3 Passing probabilities from the logistic regressions

Feature	Closest geometry to passing probability = 50%	Units
Double bends	38	degrees
Single bends	32	degrees
Step-overs	1170	meters
Gaps	24500	meters

4 Passing probability on straight section

Feature	Passing probability per meter	Stopping probability per meter
Straight segment	0.99999	0.00001

Event	Termini on straight segments/Total termini	Features at termini
1. Parkfield 1966	1/2	Bend
2. Izmit-Kocaeli	1/2	Bend
3. Landers	4/6	Bends
4. Hector Mine	0/3	Bends, step-overs, gap
5. Balochistan	1/2	Bend
6. Borrego	1/2	Bend
7. Imperial 1979	1/2	Bends, step-over
8. Superstition Hills	0/2	Step-overs, bends
9. Kobe	0/3	Bends
10. Denali	2/2	-
11. Duzce	0/2	Bends
12. Napa	0/3	Step-over, bends, gap
13. Yushu	0/2	Bends
14. Hualien	0/2	Bends
15. Darfield	0/2	Step-overs, bend
16. Galway Lake	0/2	Step-overs
17. Chalfant Valley	0/2	Bends
18. Zirkuh	1/2	Step-over
19. Ridgecrest (foreshock)	0/2	Step-overs, bend
20. Kumamoto	1/3	Bends
21. Ridgecrest (mainshock)	0/2	Step-over, bends
22. Imperial 1940	0/2	Step-overs, bends
23. San Miguel	0/2	Step-overs, bend
24. Yutian	1/2	Bend
25. Luzon	0/2	Bends, step-over, gap
26. Elmore Ranch	0/2	Bends
27. Pisayambo	0/2	Step-overs, bends
28. Izu Peninsula	0/2	Bends
29. Izu Oshima	1/2	Bend
30. Neftegorsk	0/2	Bends
31. Parkfield 2004	1/2	Bend
All events	**16/70**	-

Table 1: Number of termini on straight fault segments and on earthquake gates for the events on the FDHI database.


Earthquake gate types
stepover breached
stepover unbreached
bend breached
bend unbreached
strand breached
splay breached
splay unbreached
gap breached
gap unbreached

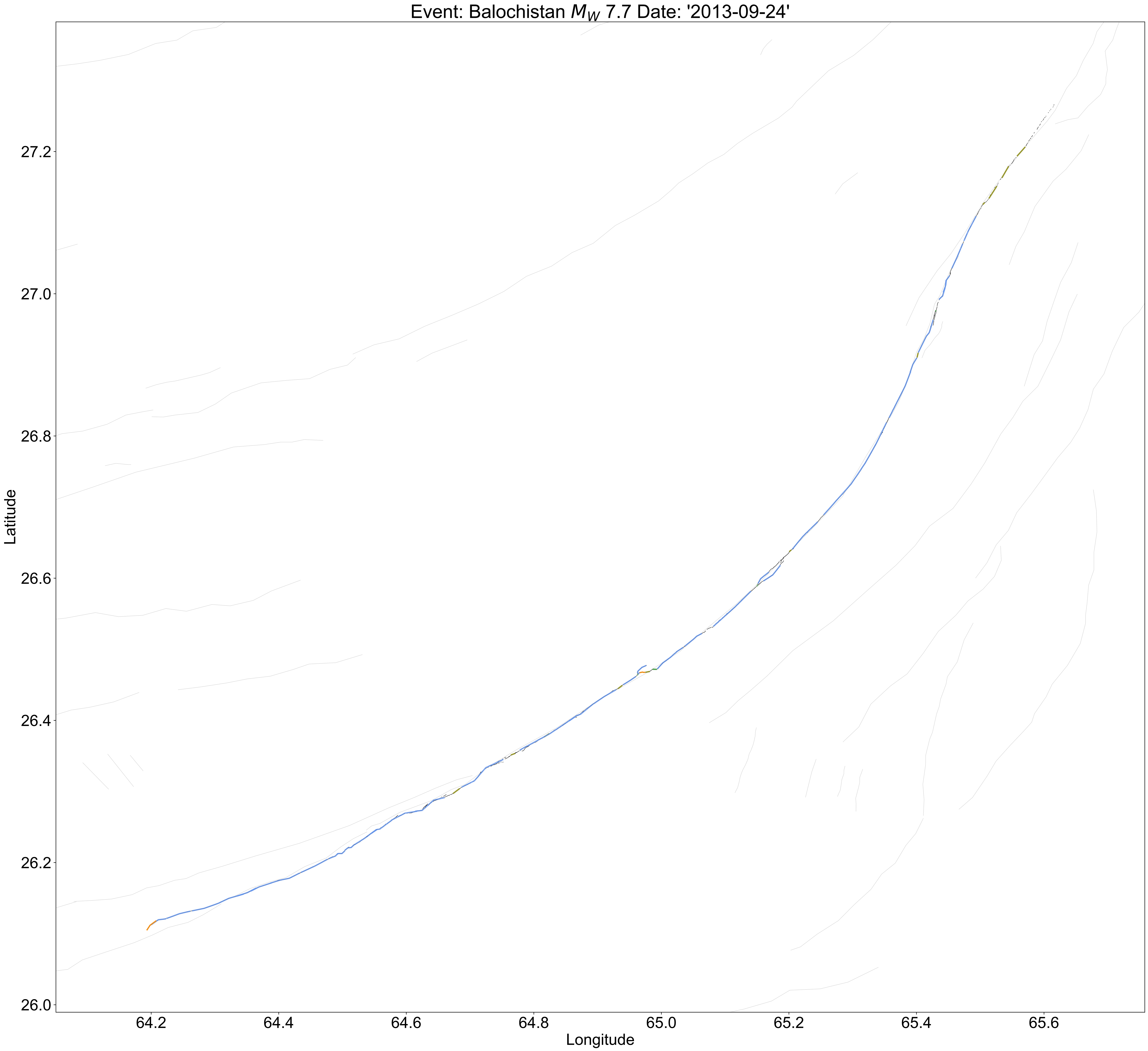
Event: Balochistan M_W 7.7 Date: '2013-09-24'
Latitude
27.2
27.0
26.8
26.6
26.4
26.2
26.0
Longitude
64.2
64.4
64.6
64.8
65.0
65.2
65.4
65.6

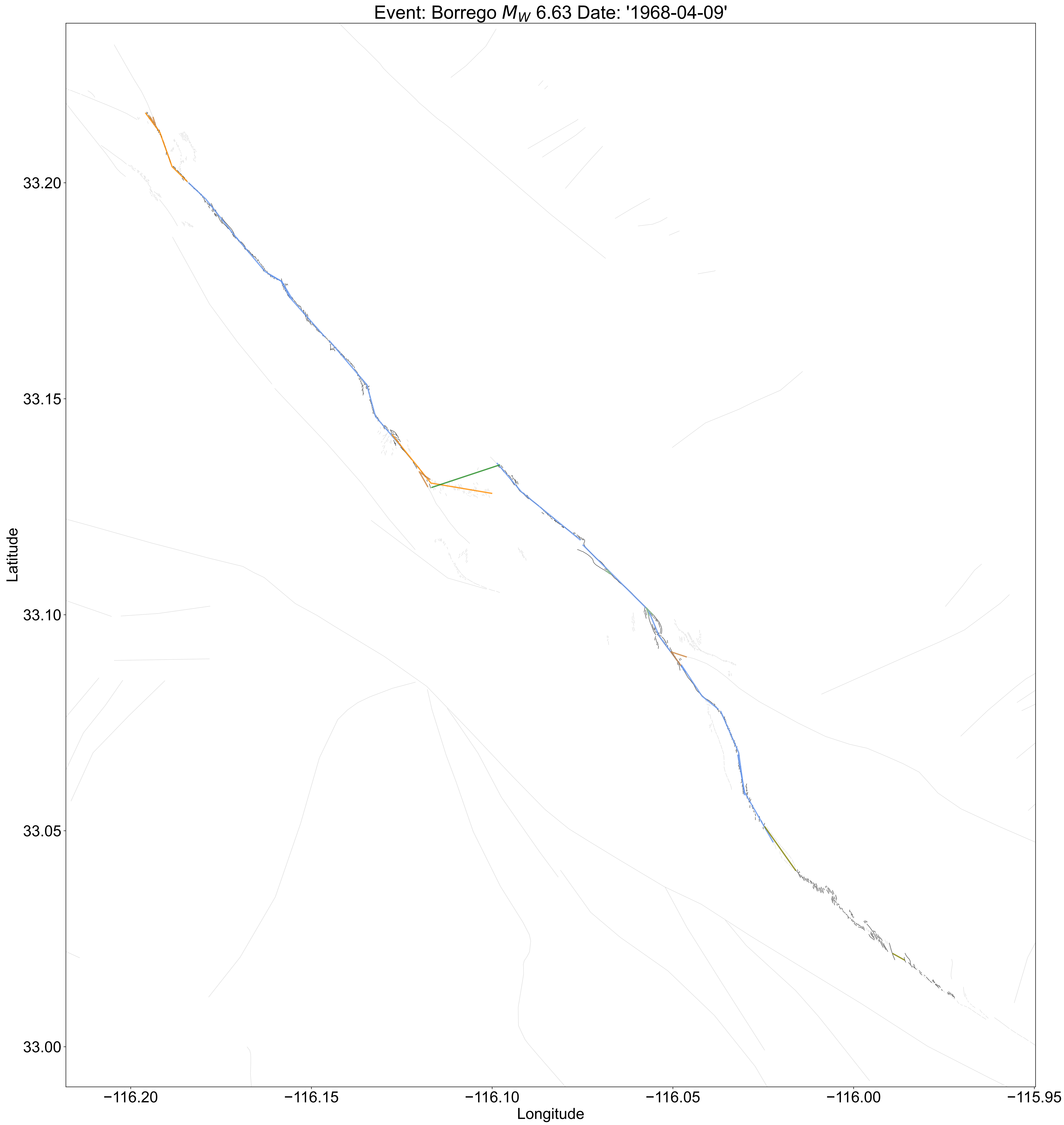

Event: Borrego M_W 6.63 Date: '1968-04-09'
Latitude
Longitude
33.20
33.15
33.10
33.05
33.00
−116.20
−116.15
−116.10
−116.05
−116.00
−115.95

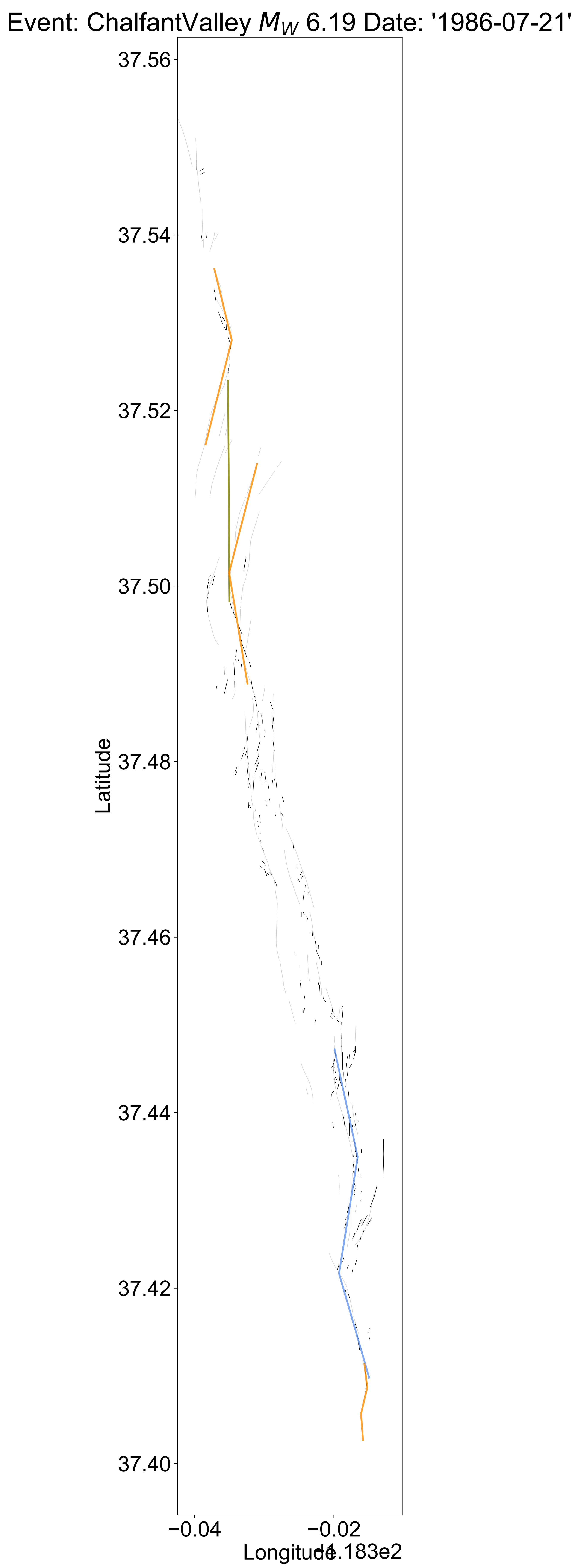

Event: ChalfantValley M_W 6.19 Date: '1986-07-21'
37.56
37.54
37.52
37.50
37.48
37.46
37.44
37.42
37.40
Latitude
−0.04
−0.02
Longitude
−1.183e2

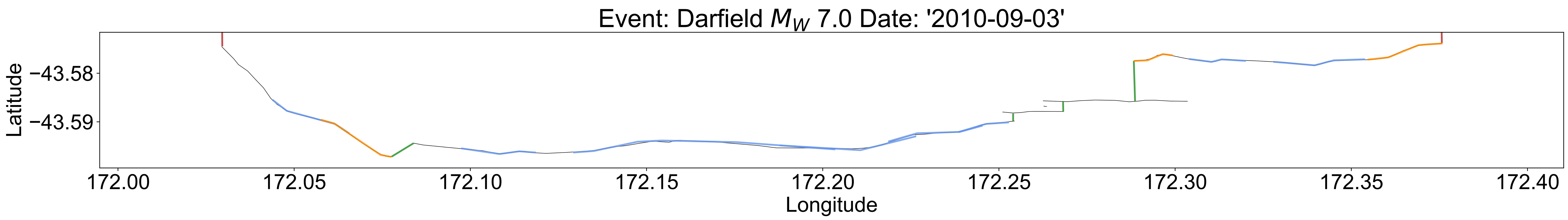

Event: Darfield M_W 7.0 Date: '2010-09-03'
Latitude
−43.58
−43.59
Longitude
172.00
172.05
172.10
172.15
172.20
172.25
172.30
172.35
172.40

Event: Denali M_W 7.9 Date: '2002-11-03'

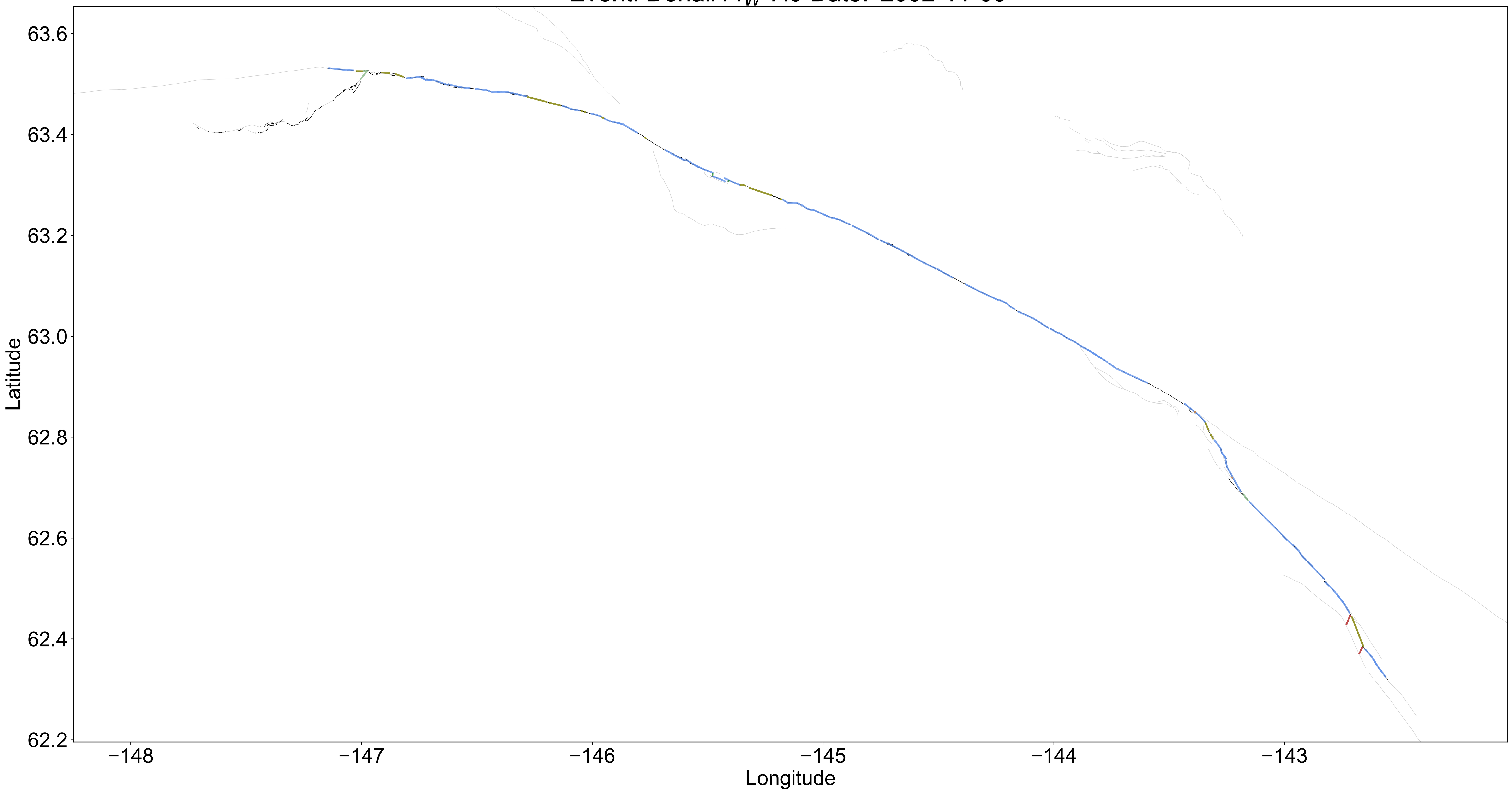

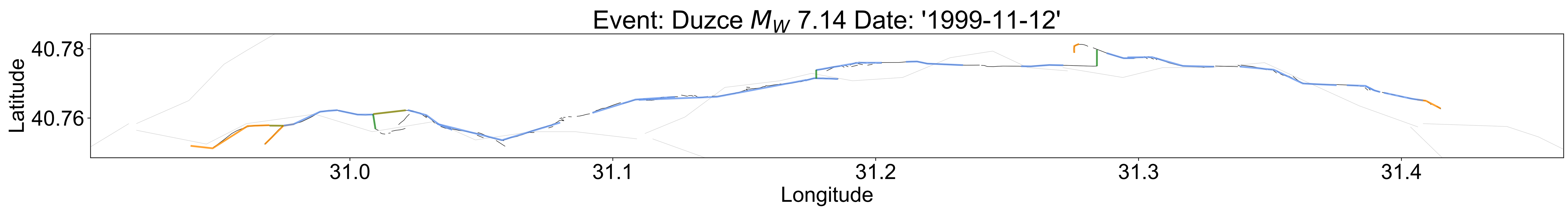

Event: Duzce M_W 7.14 Date: '1999-11-12'
40.78
40.76
Latitude
31.0
31.1
31.2
31.3
31.4
Longitude

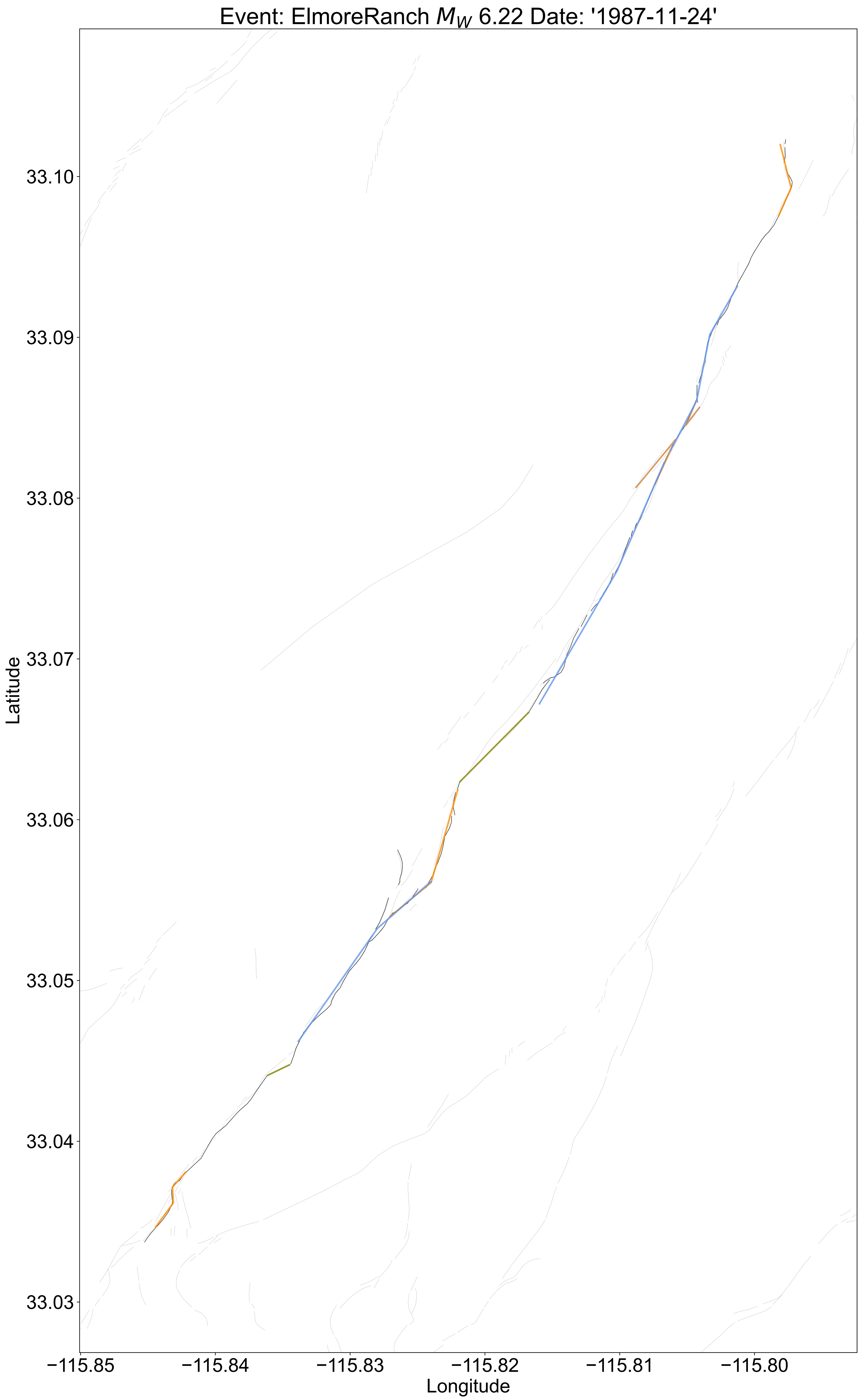

Event: ElmoreRanch M_W 6.22 Date: '1987-11-24'
Latitude
33.10
33.09
33.08
33.07
33.06
33.05
33.04
33.03
−115.85
−115.84
−115.83
−115.82
−115.81
−115.80
Longitude

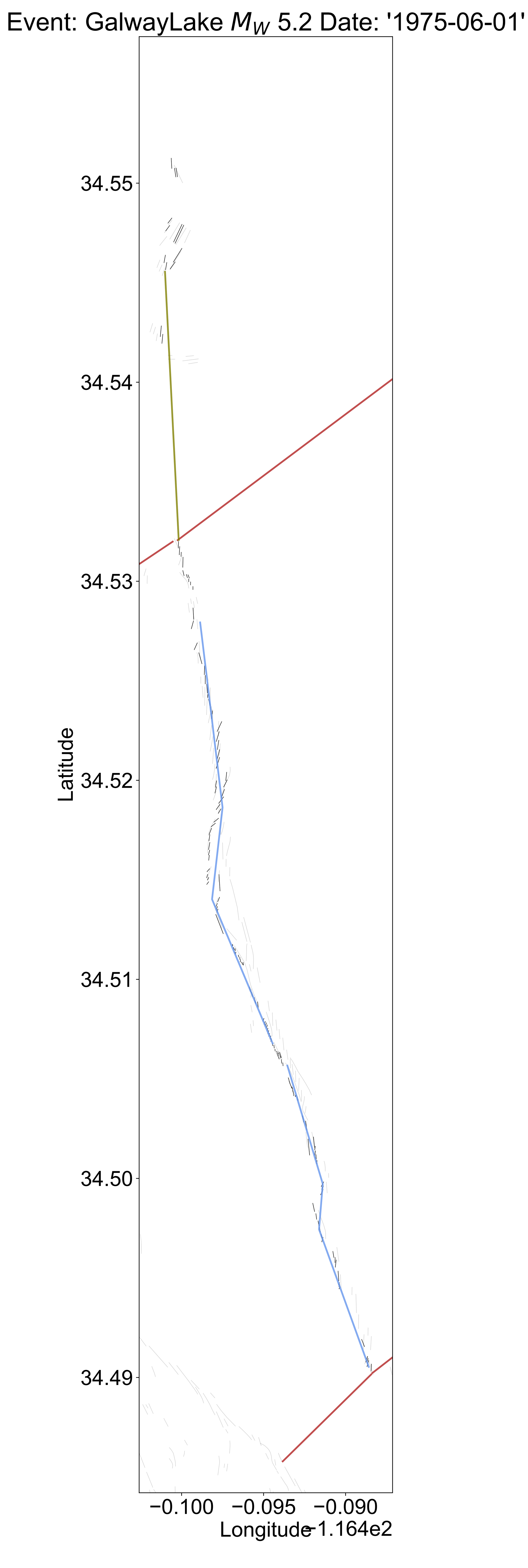

Event: GalwayLake M_W 5.2 Date: '1975-06-01'
34.55
34.54
34.53
34.52
34.51
34.50
34.49
Latitude
−0.100
−0.095
−0.090
Longitude
−1.164e2

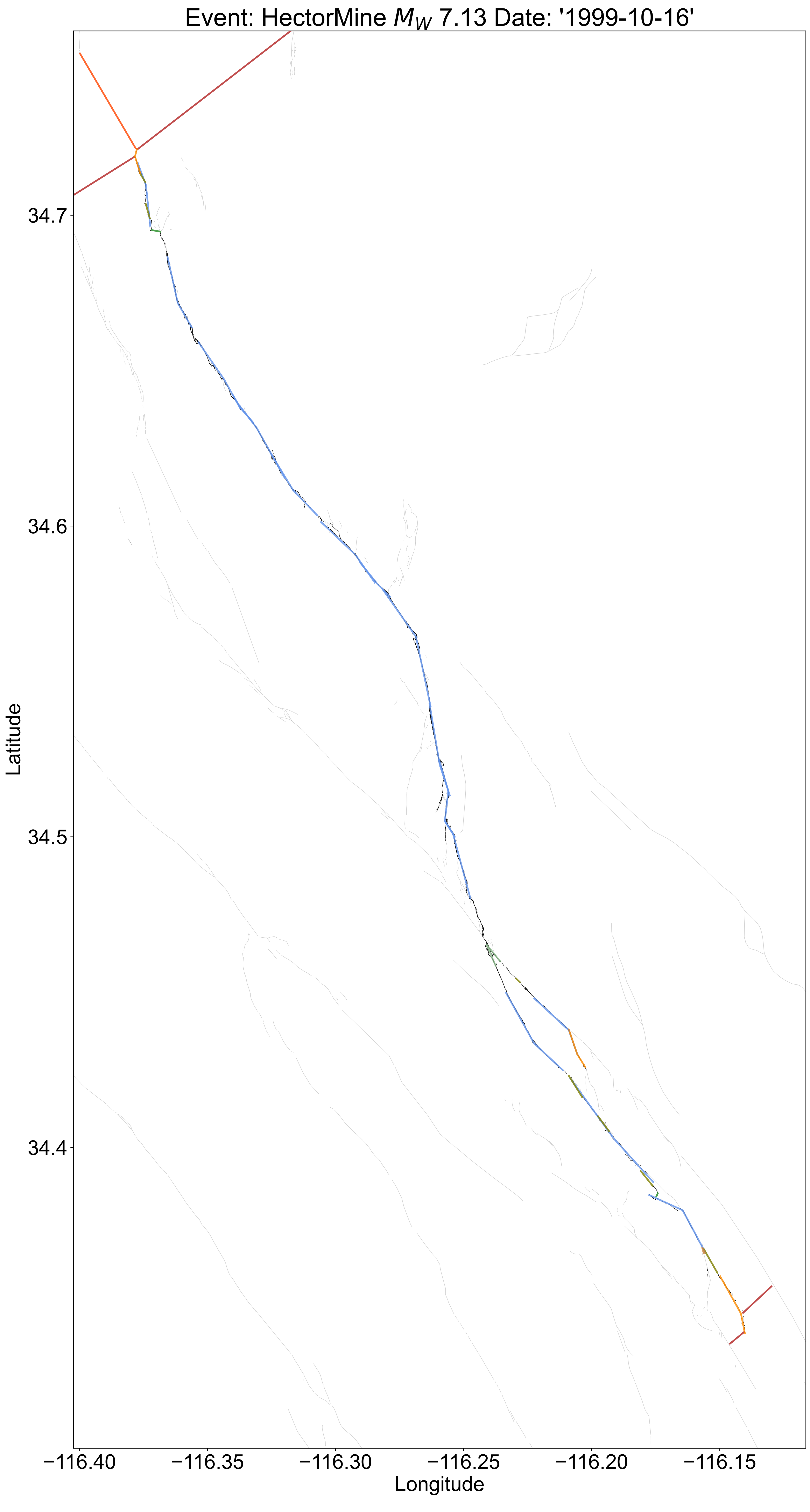

Event: HectorMine M_W 7.13 Date: '1999-10-16'
34.7
34.6
34.5
34.4
Latitude
−116.40
−116.35
−116.30
−116.25
−116.20
−116.15
Longitude

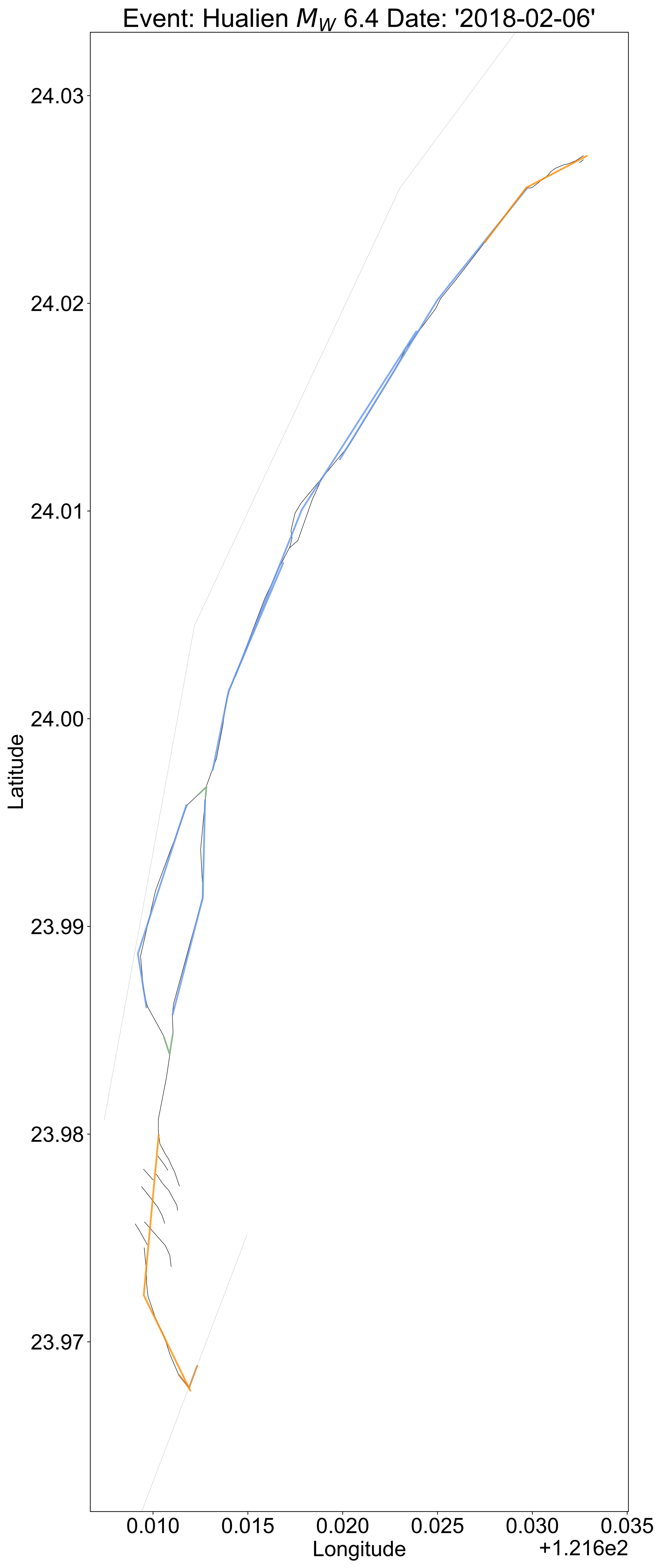

Event: Hualien M_W 6.4 Date: '2018-02-06'
Latitude
Longitude
24.03
24.02
24.01
24.00
23.99
23.98
23.97
0.010
0.015
0.020
0.025
0.030
0.035
+1.216e2

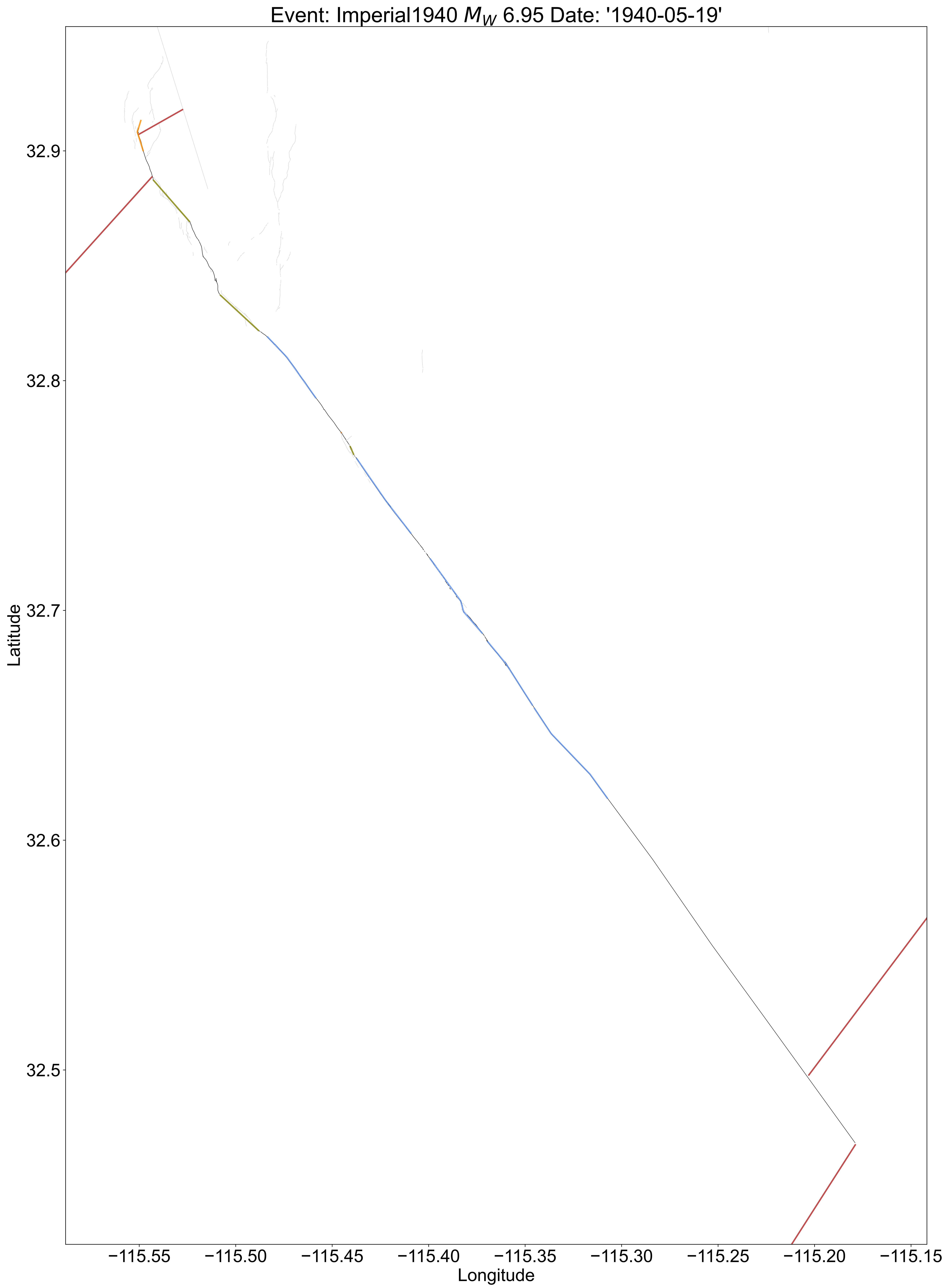

Event: Imperial1940 M_W 6.95 Date: '1940-05-19'
Latitude
Longitude
32.9
32.8
32.7
32.6
32.5
−115.55
−115.50
−115.45
−115.40
−115.35
−115.30
−115.25
−115.20
−115.15

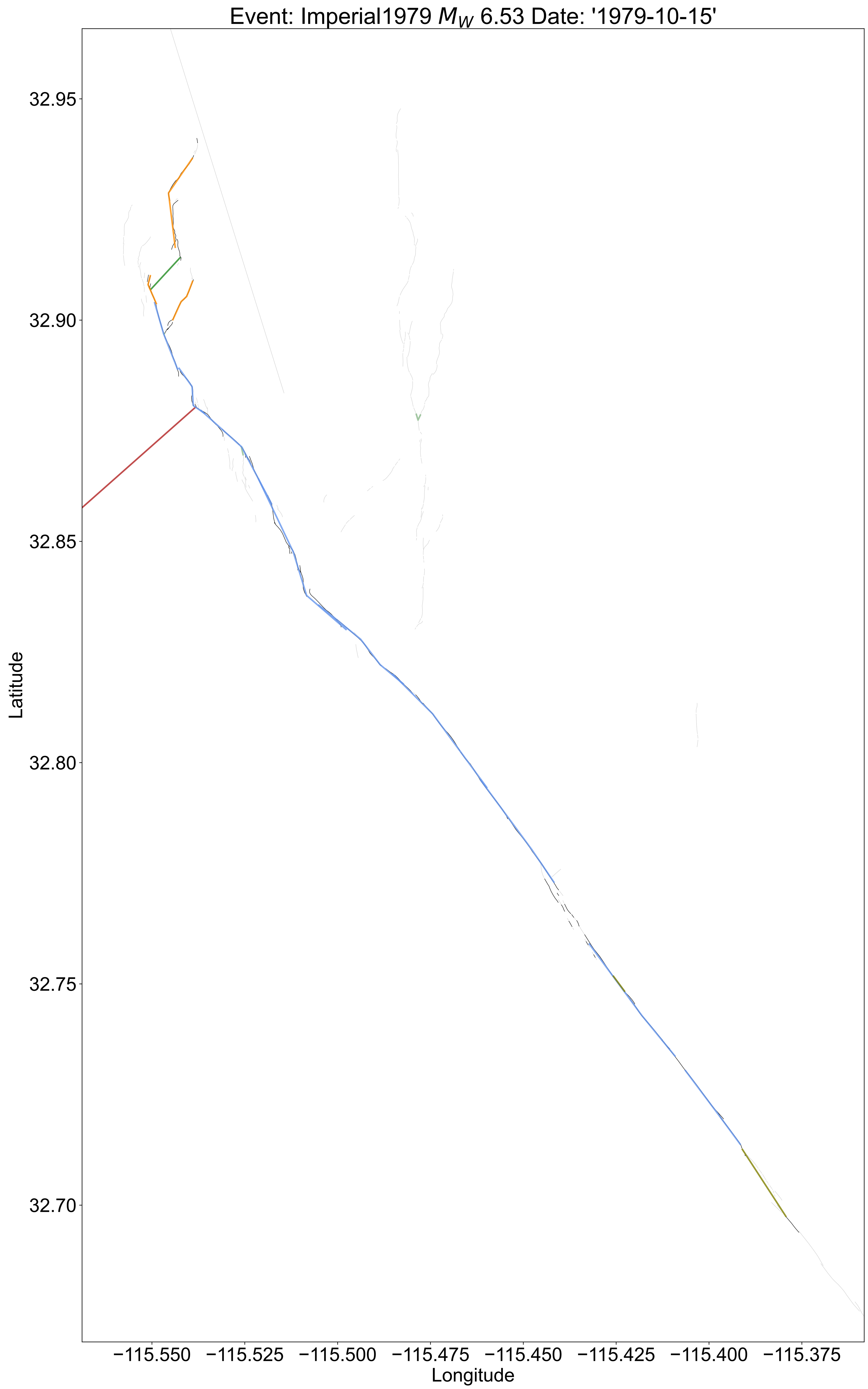
Event: Imperial1979 M_W 6.53 Date: '1979-10-15'
Latitude
32.95
32.90
32.85
32.80
32.75
32.70
Longitude
−115.550
−115.525
−115.500
−115.475
−115.450
−115.425
−115.400
−115.375

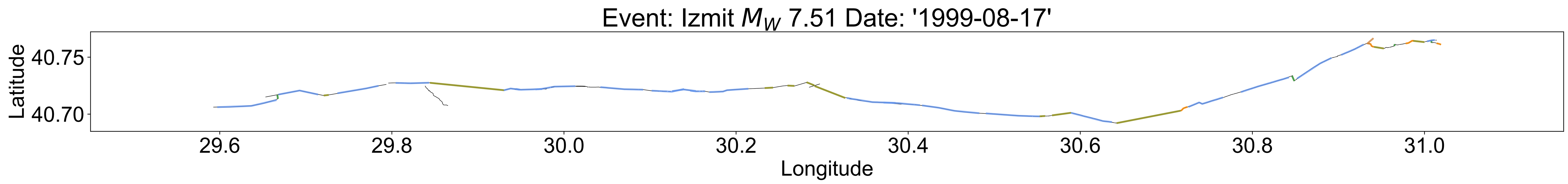
Event: Izmit M_W 7.51 Date: '1999-08-17'
Latitude
40.75
40.70
29.6
29.8
30.0
30.2
30.4
30.6
30.8
31.0
Longitude

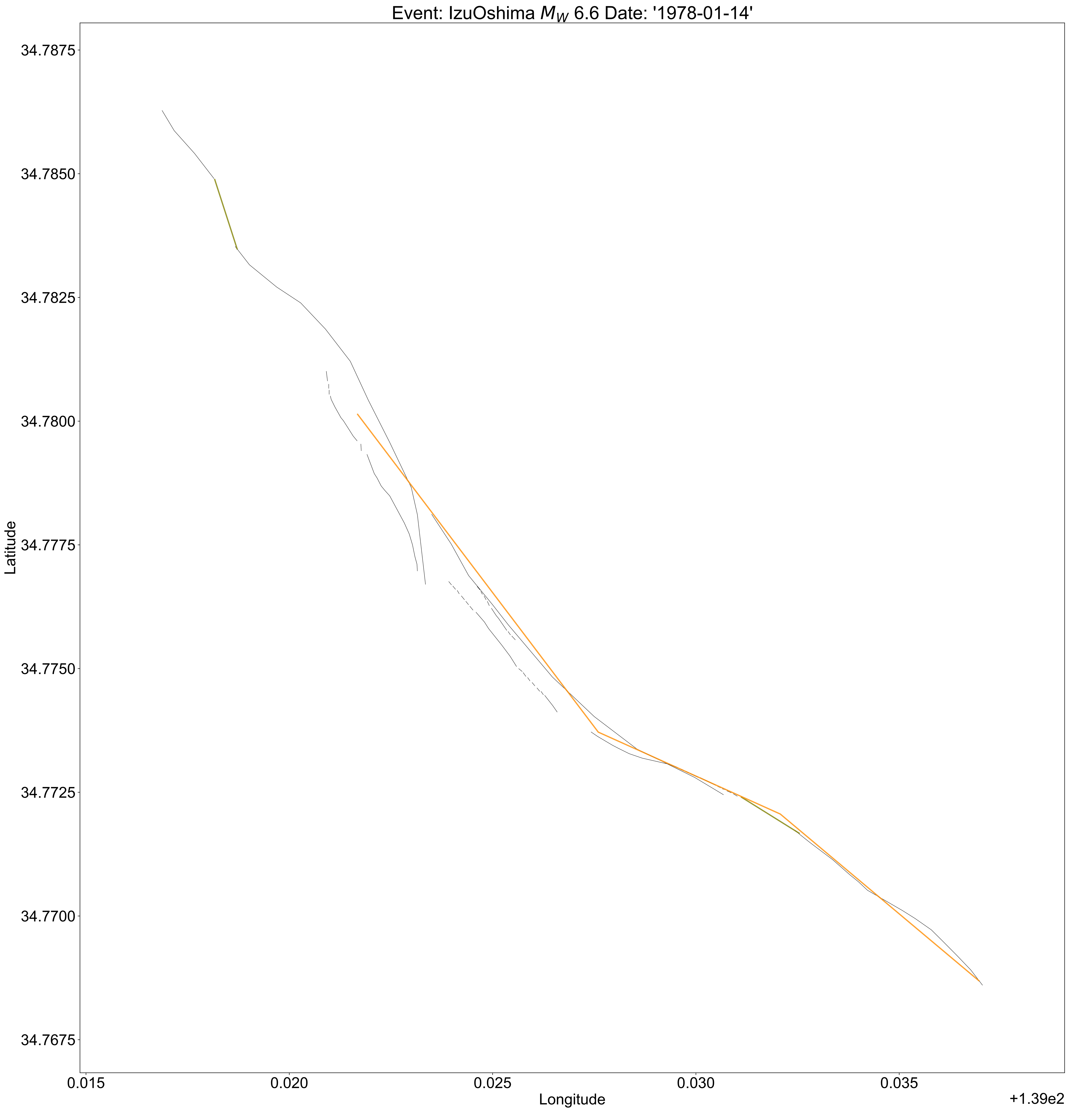

Event: IzuOshima M_W 6.6 Date: '1978-01-14'
34.7875
34.7850
34.7825
34.7800
34.7775
34.7750
34.7725
34.7700
34.7675
Latitude
0.015
0.020
0.025
0.030
0.035
+1.39e2
Longitude

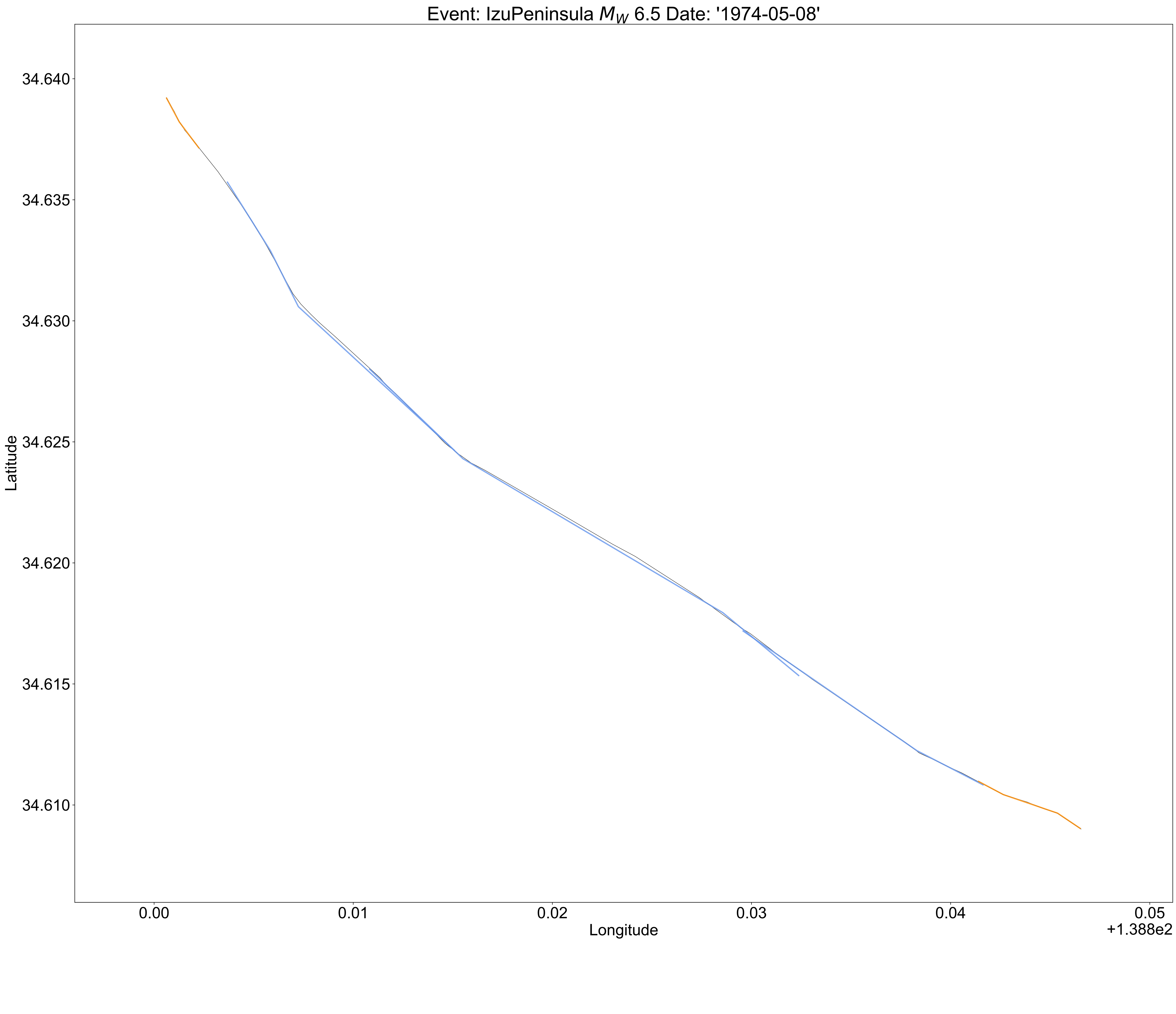

Event: IzuPeninsula M_W 6.5 Date: '1974-05-08'
34.640
34.635
34.630
34.625
34.620
34.615
34.610
Latitude
0.00
0.01
0.02
0.03
0.04
0.05
+1.388e2
Longitude

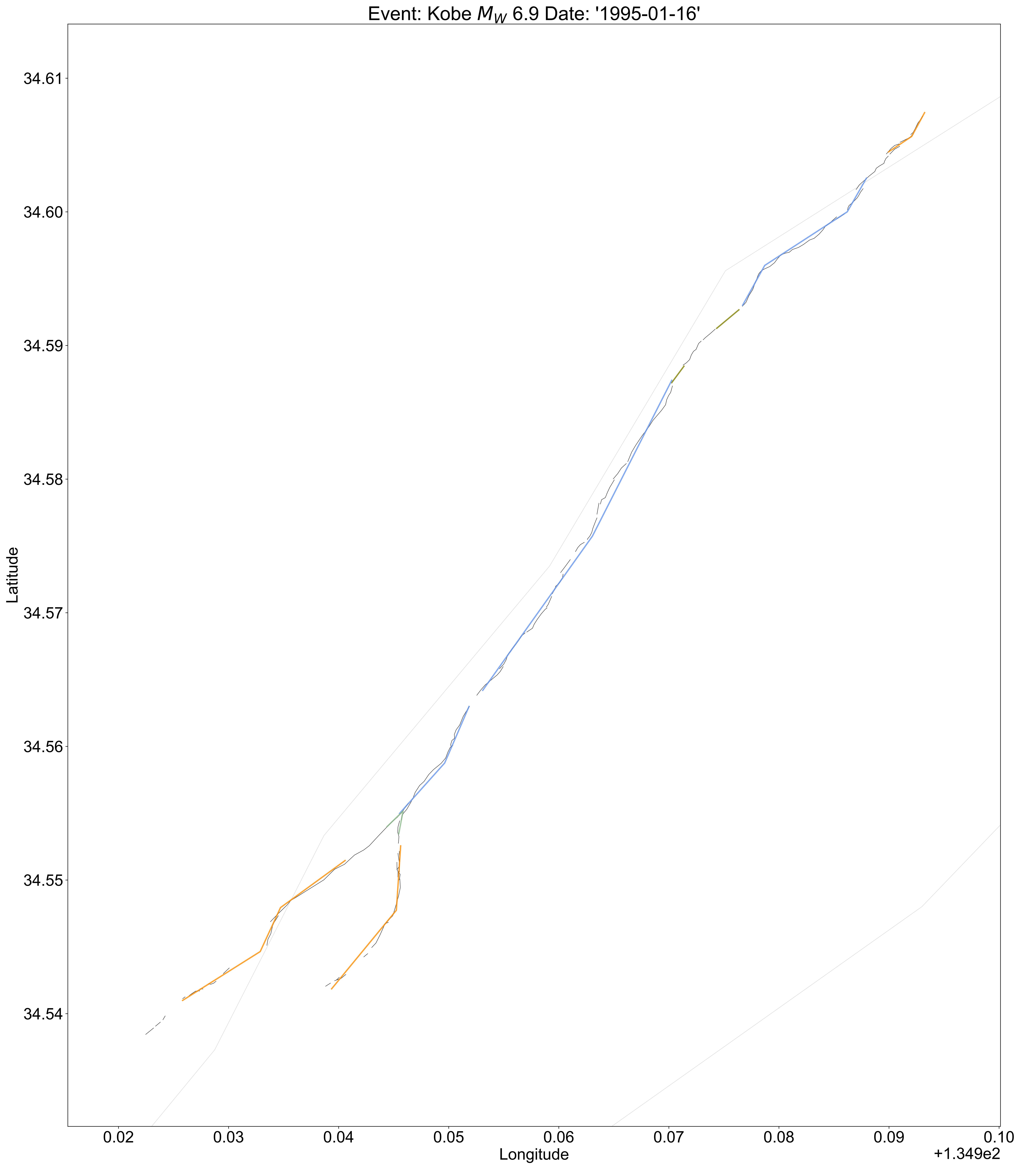

Event: Kobe M_W 6.9 Date: '1995-01-16'
Latitude
Longitude
34.61
34.60
34.59
34.58
34.57
34.56
34.55
34.54
0.02
0.03
0.04
0.05
0.06
0.07
0.08
0.09
0.10
+1.349e2

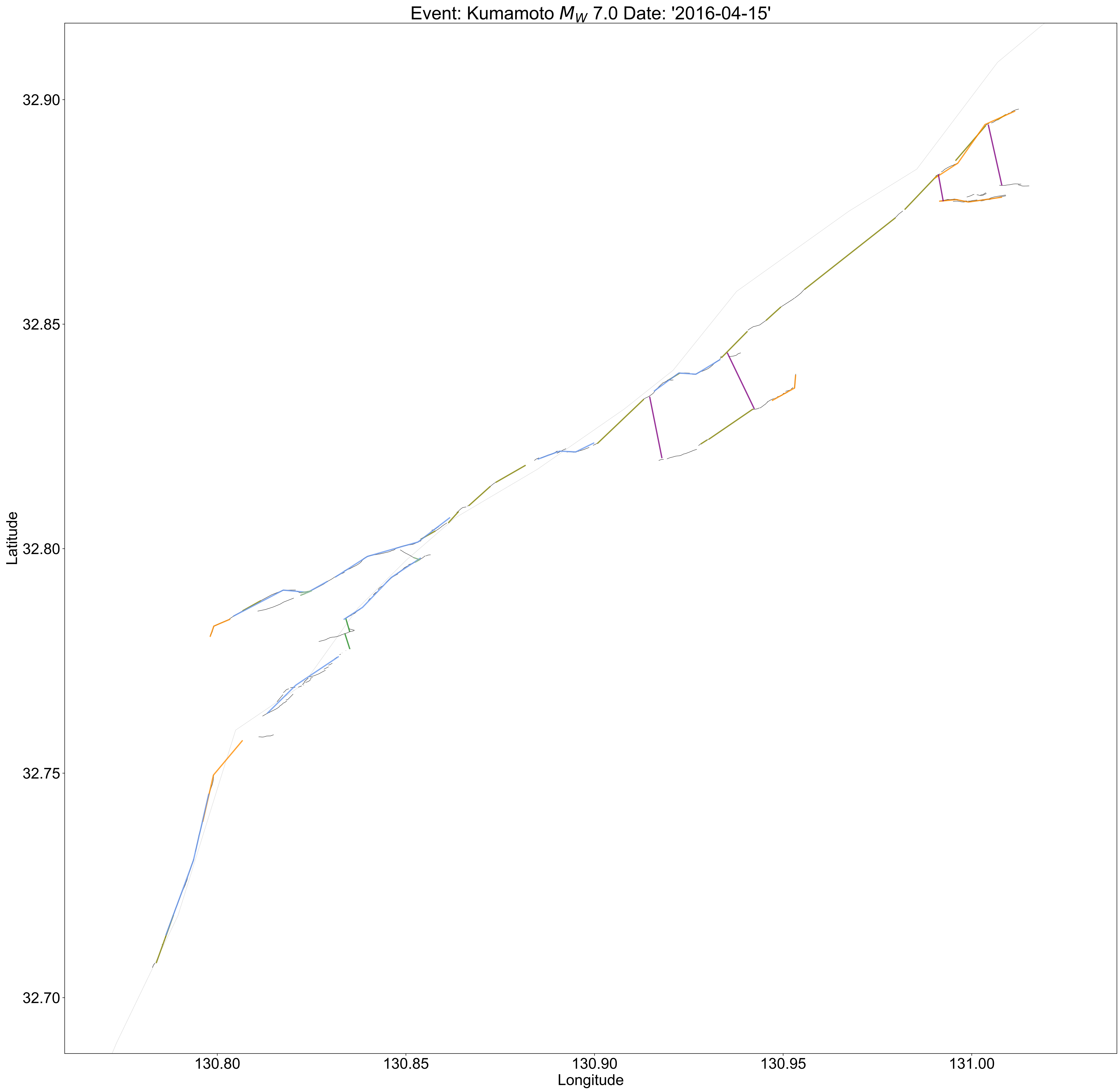
Event: Kumamoto M_W 7.0 Date: '2016-04-15'
32.90
32.85
32.80
32.75
32.70
Latitude
130.80
130.85
130.90
130.95
131.00
Longitude

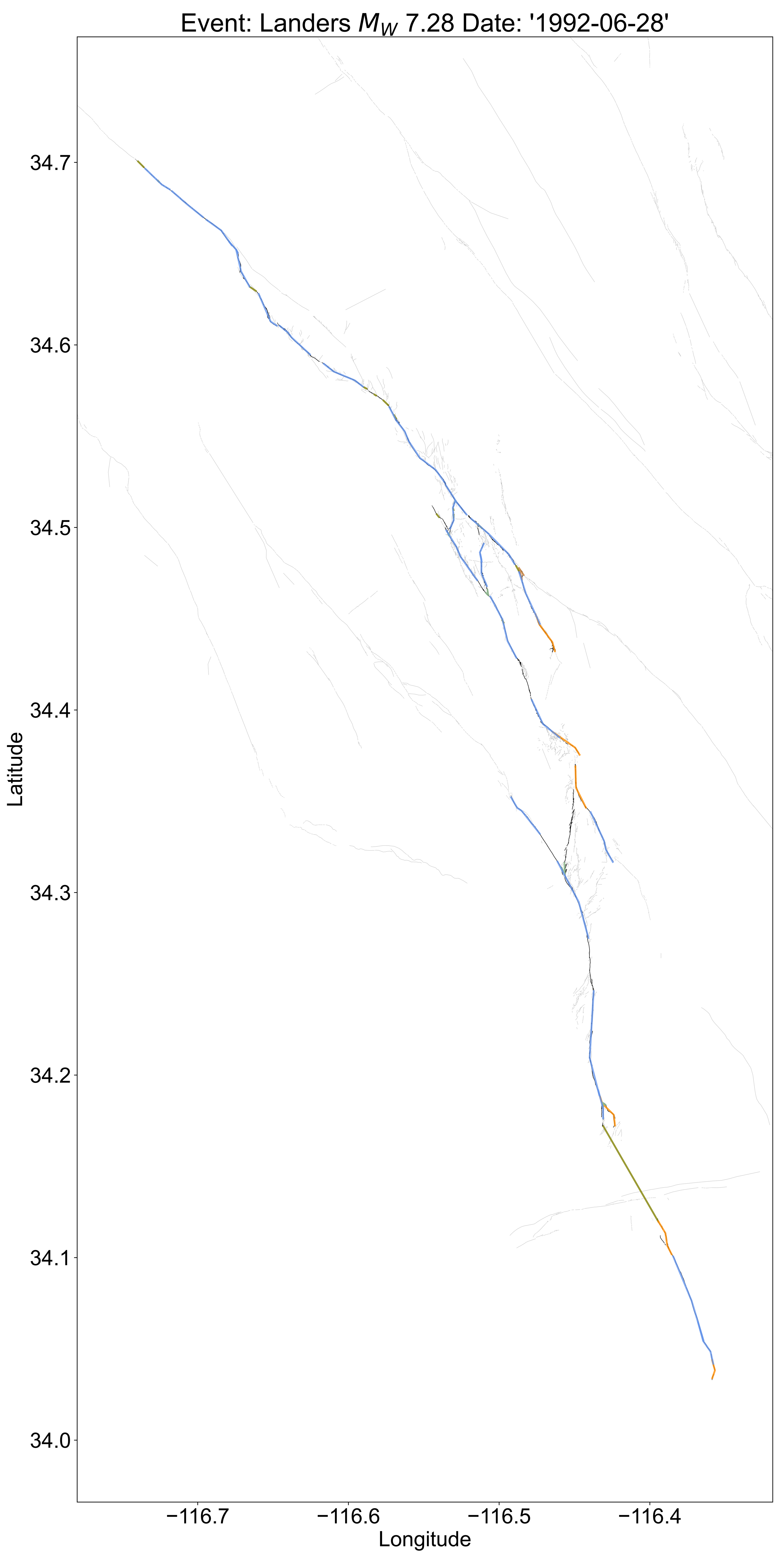

Event: Landers M_W 7.28 Date: '1992-06-28'
34.7
34.6
34.5
34.4
34.3
34.2
34.1
34.0
Latitude
−116.7
−116.6
−116.5
−116.4
Longitude

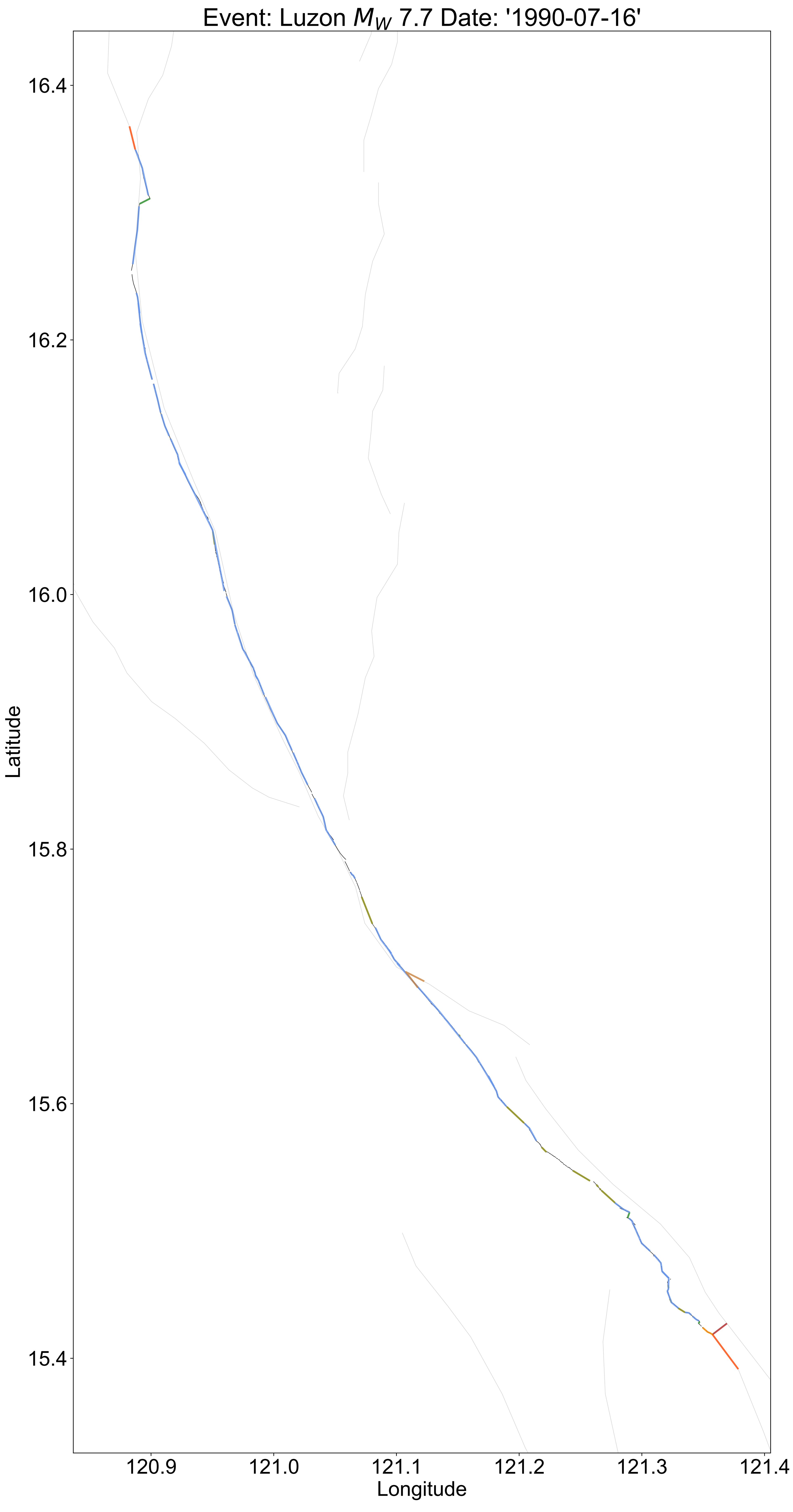
Event: Luzon M_W 7.7 Date: '1990-07-16'
16.4
16.2
16.0
15.8
15.6
15.4
Latitude
120.9
121.0
121.1
121.2
121.3
121.4
Longitude

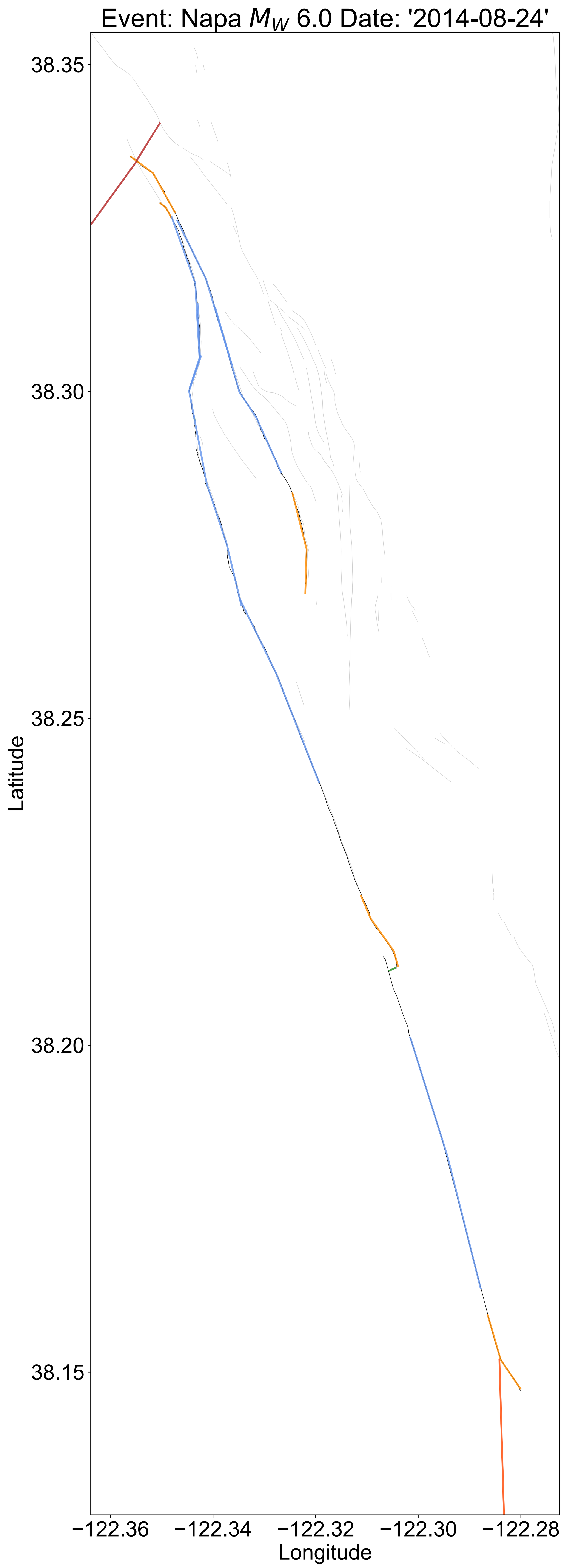
Event: Napa M_W 6.0 Date: '2014-08-24'
Latitude
Longitude
38.35
38.30
38.25
38.20
38.15
−122.36
−122.34
−122.32
−122.30
−122.28

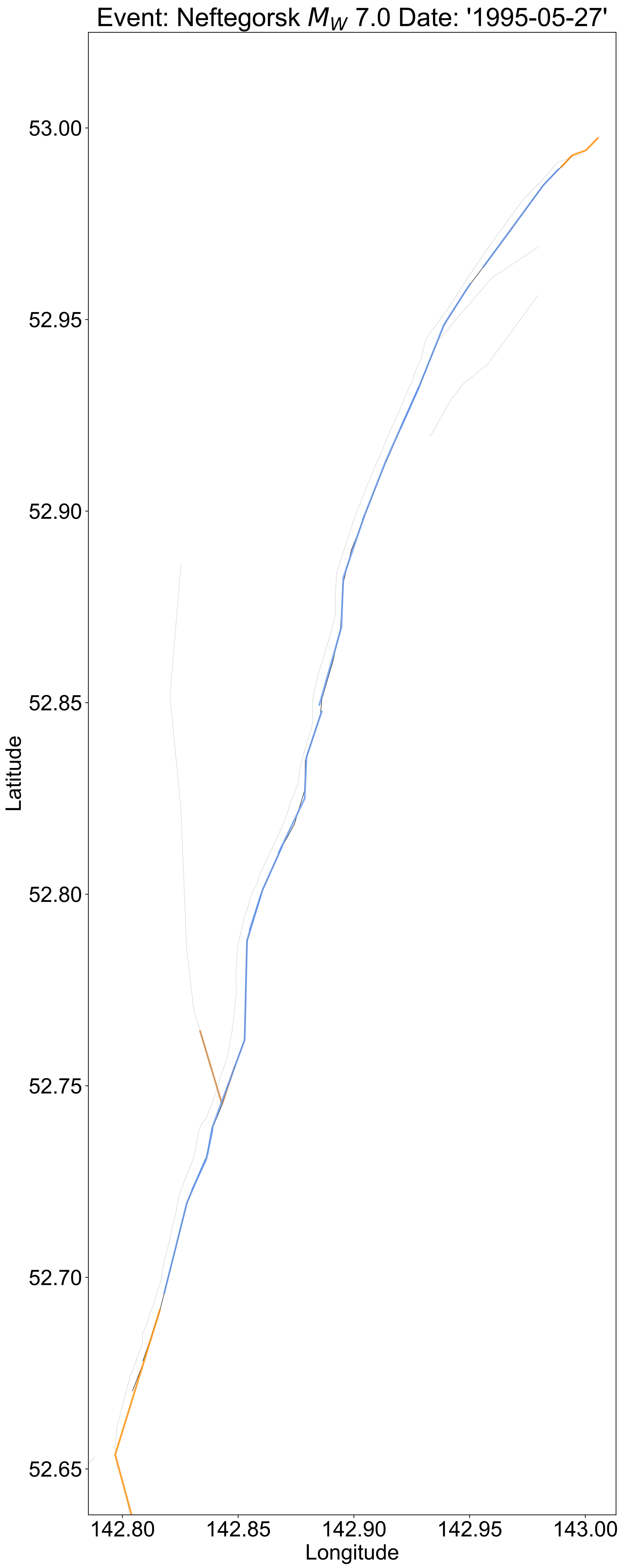

Event: Neftegorsk M_W 7.0 Date: '1995-05-27'
Latitude
Longitude
53.00
52.95
52.90
52.85
52.80
52.75
52.70
52.65
142.80
142.85
142.90
142.95
143.00

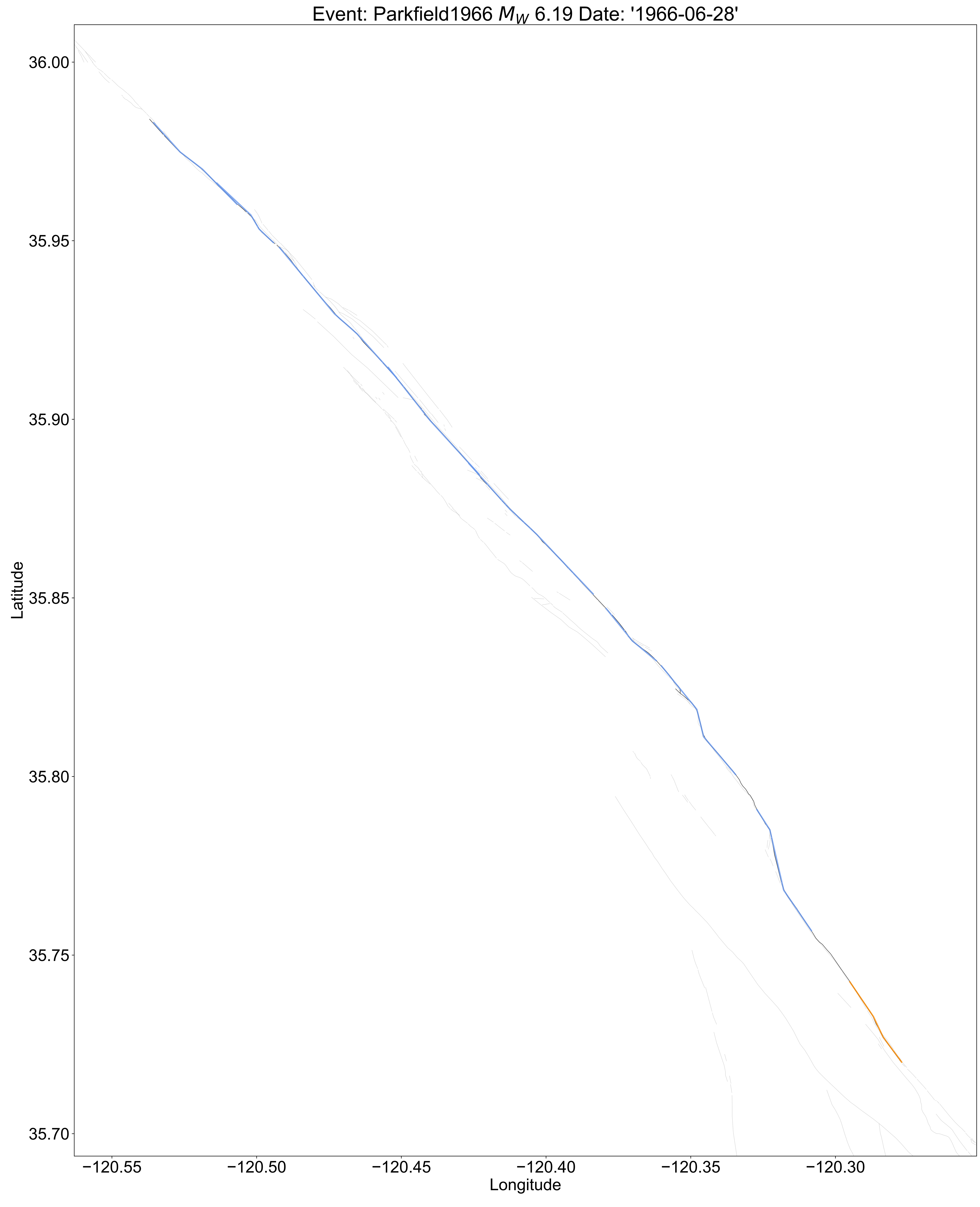
Event: Parkfield1966 M_W 6.19 Date: '1966-06-28'
Latitude
36.00
35.95
35.90
35.85
35.80
35.75
35.70
−120.55
−120.50
−120.45
−120.40
−120.35
−120.30
Longitude

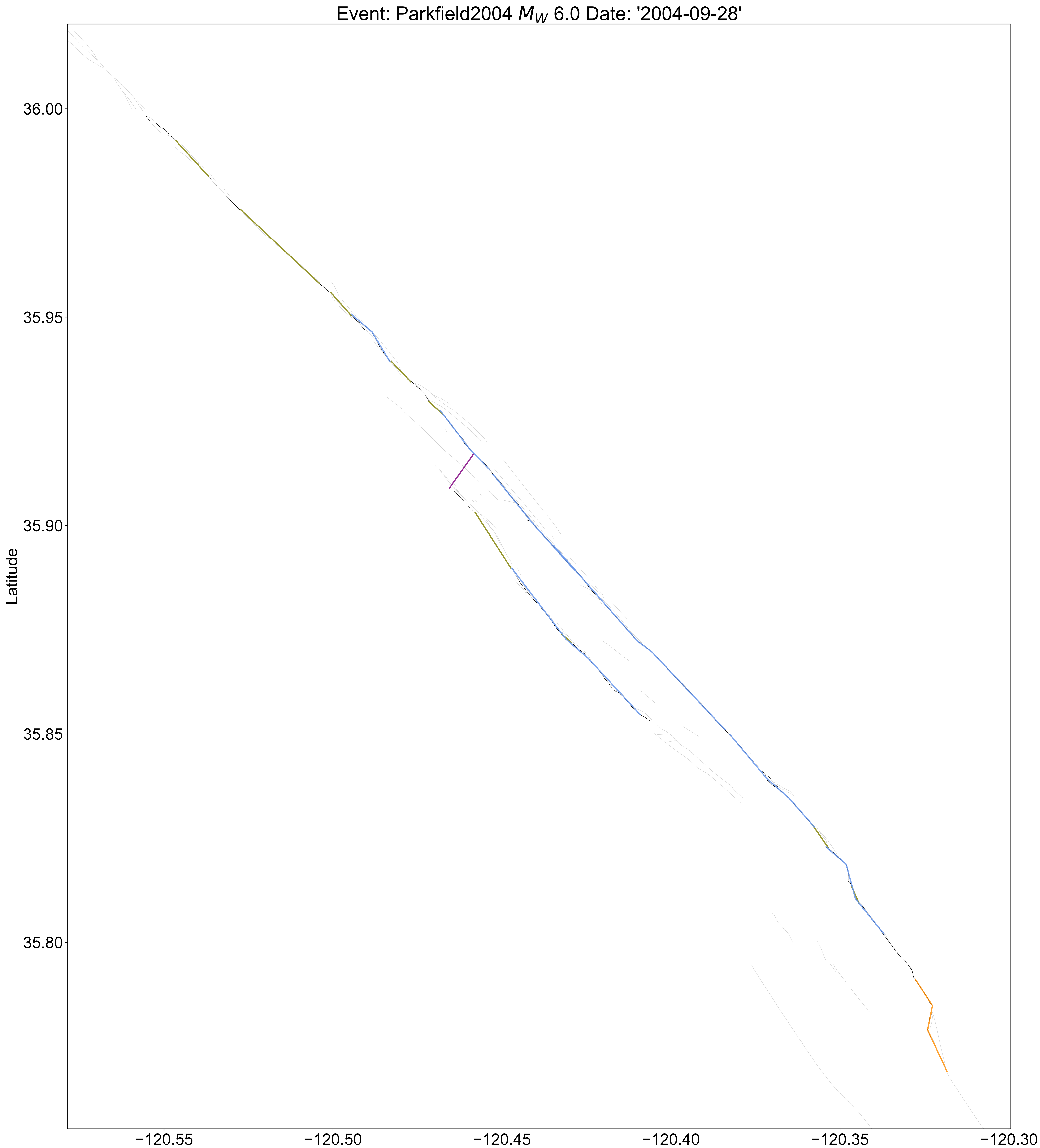

Event: Parkfield2004 M_W 6.0 Date: '2004-09-28'
36.00
35.95
35.90
35.85
35.80
Latitude
−120.55
−120.50
−120.45
−120.40
−120.35
−120.30
Longitude

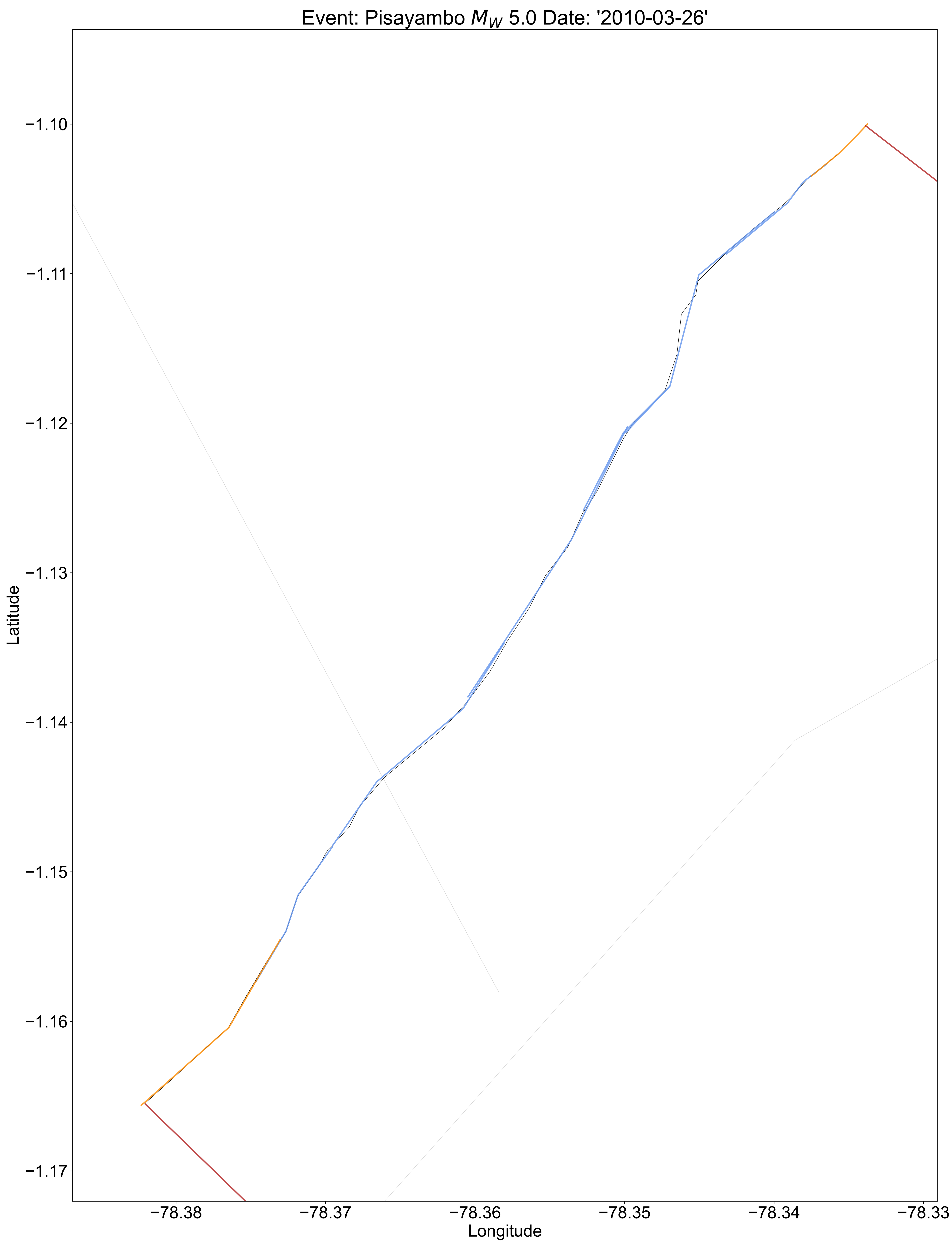
Event: Pisayambo M_W 5.0 Date: '2010-03-26'
Latitude
−1.10
−1.11
−1.12
−1.13
−1.14
−1.15
−1.16
−1.17
Longitude
−78.38
−78.37
−78.36
−78.35
−78.34
−78.33

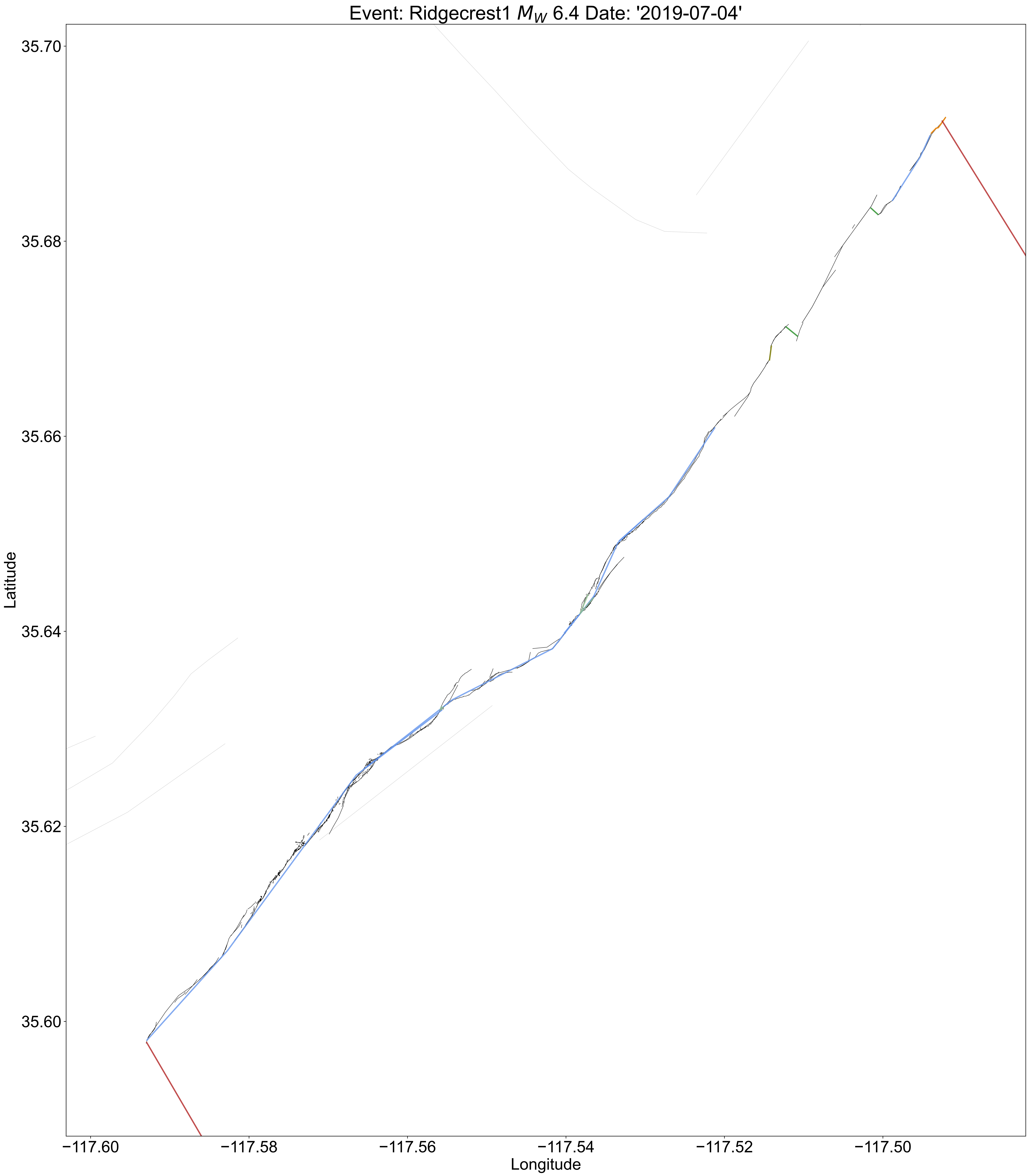
Event: Ridgecrest1 M_W 6.4 Date: '2019-07-04'
Latitude
35.70
35.68
35.66
35.64
35.62
35.60
Longitude
−117.60
−117.58
−117.56
−117.54
−117.52
−117.50

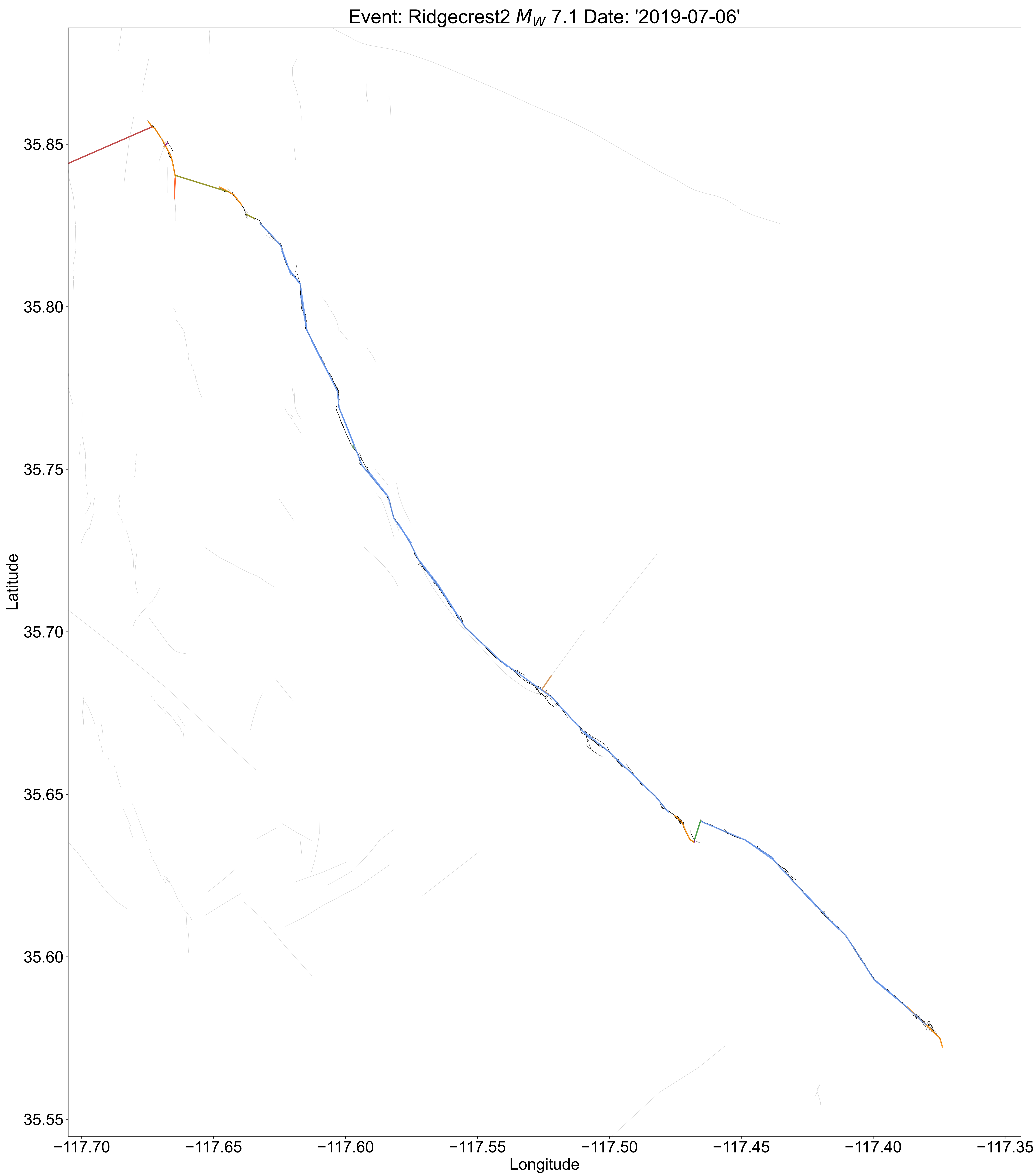
Event: Ridgecrest2 M_W 7.1 Date: '2019-07-06'
Latitude
Longitude
35.85
35.80
35.75
35.70
35.65
35.60
35.55
−117.70
−117.65
−117.60
−117.55
−117.50
−117.45
−117.40
−117.35

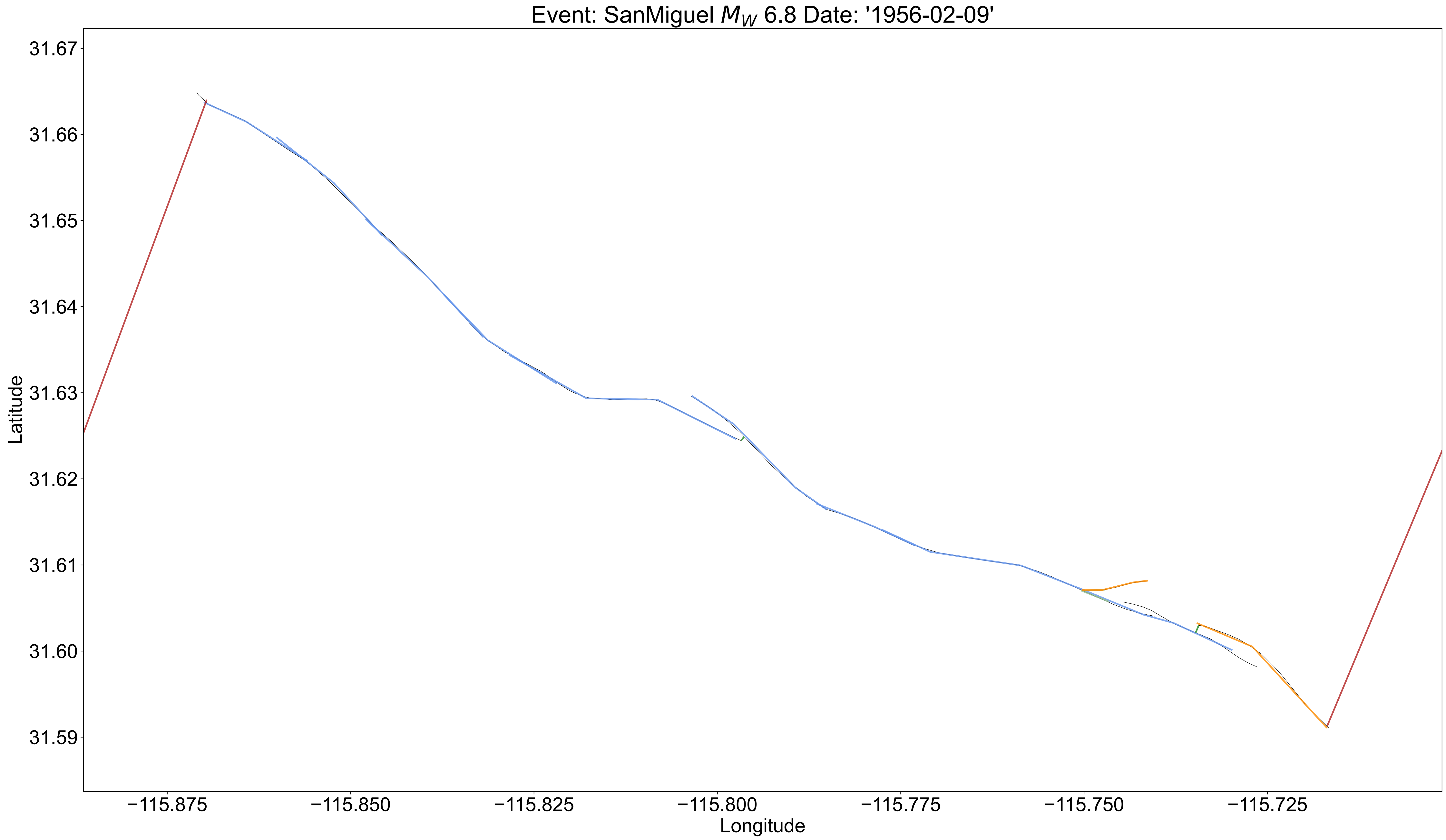
Event: SanMiguel M_W 6.8 Date: '1956-02-09'
Latitude
Longitude
31.67
31.66
31.65
31.64
31.63
31.62
31.61
31.60
31.59
−115.875
−115.850
−115.825
−115.800
−115.775
−115.750
−115.725

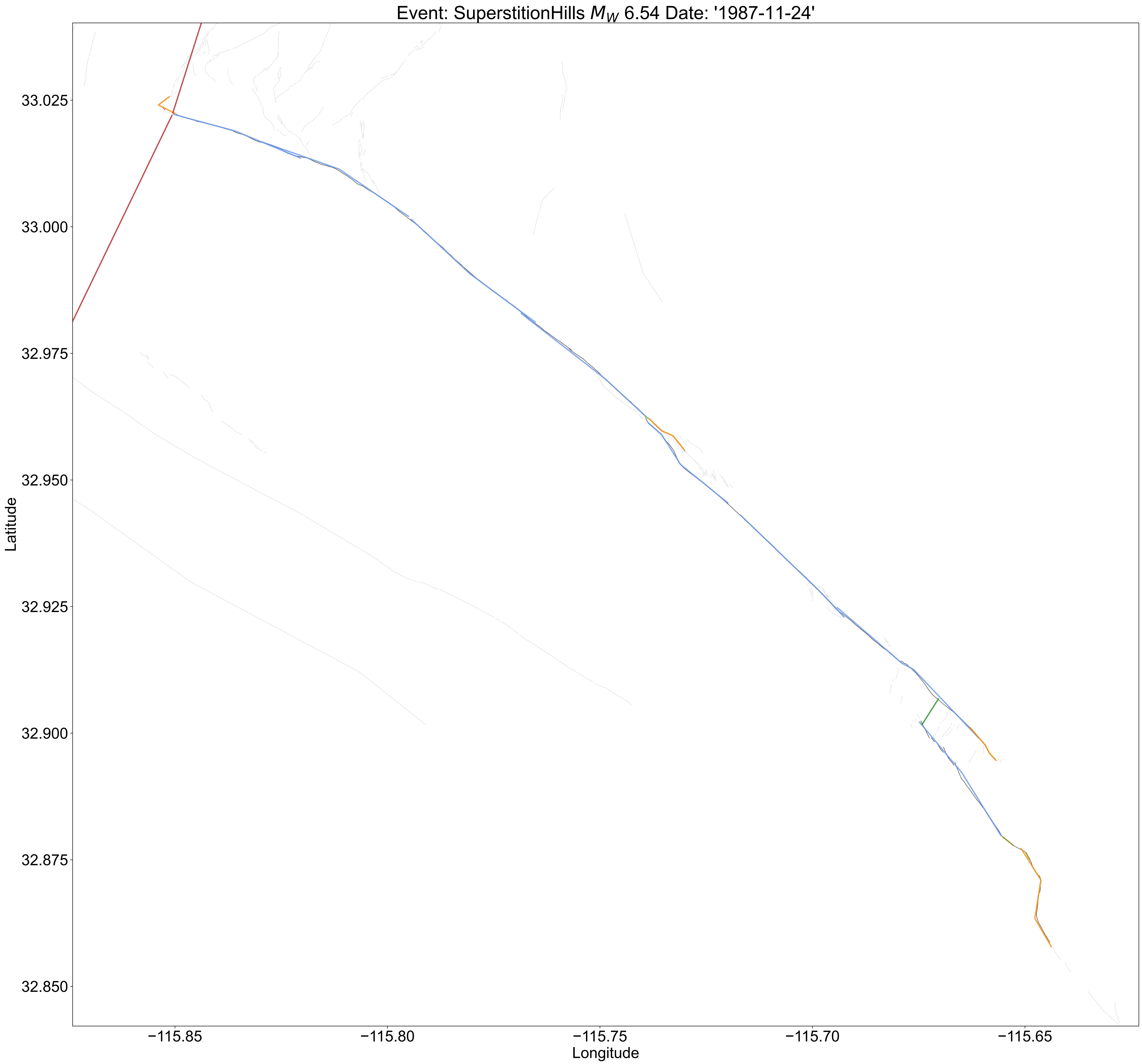

Event: SuperstitionHills M_W 6.54 Date: '1987-11-24'
33.025
33.000
32.975
32.950
32.925
32.900
32.875
32.850
Latitude
−115.85
−115.80
−115.75
−115.70
−115.65
Longitude

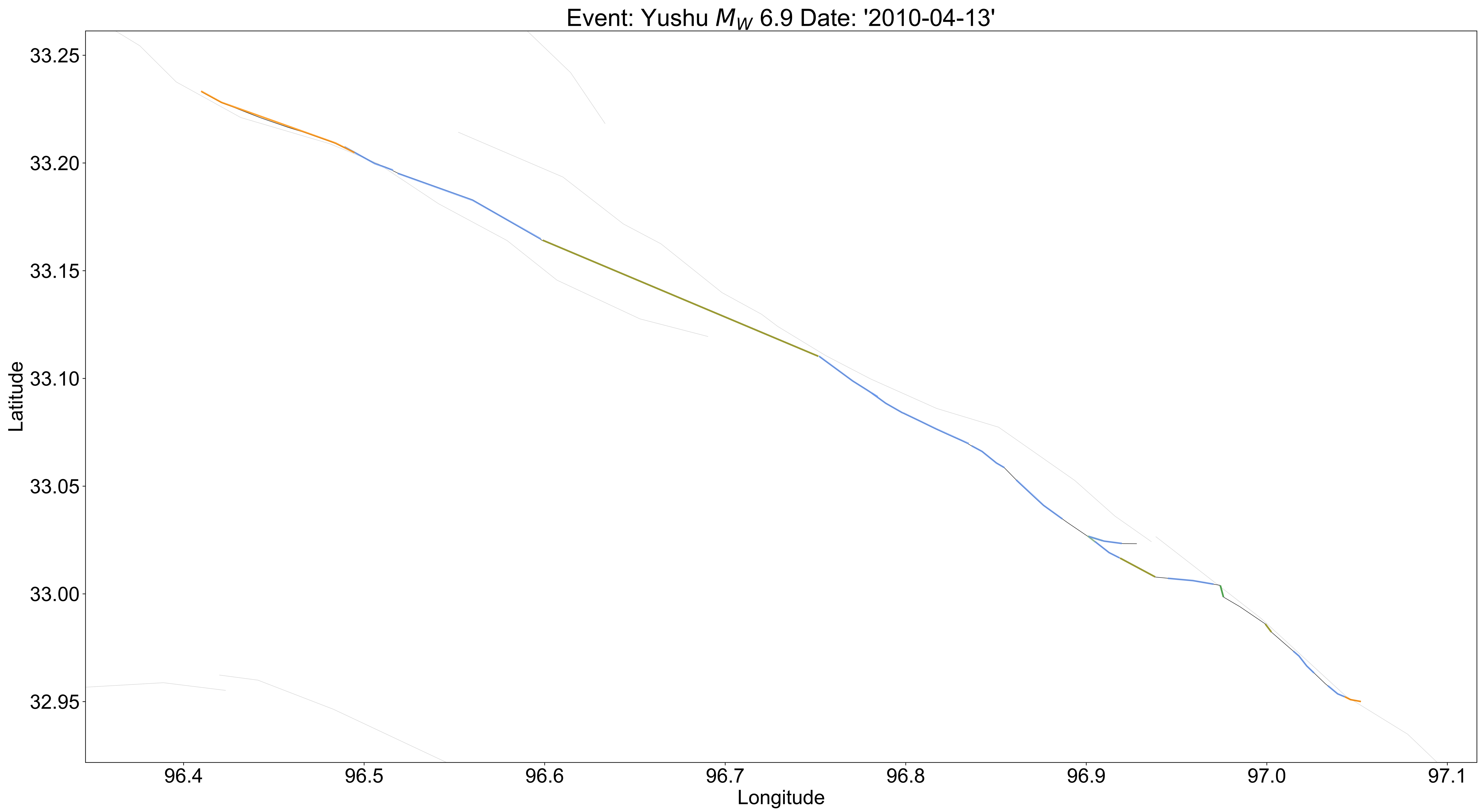
Event: Yushu M_W 6.9 Date: '2010-04-13'
33.25
33.20
33.15
33.10
33.05
33.00
32.95
Latitude
96.4
96.5
96.6
96.7
96.8
96.9
97.0
97.1
Longitude

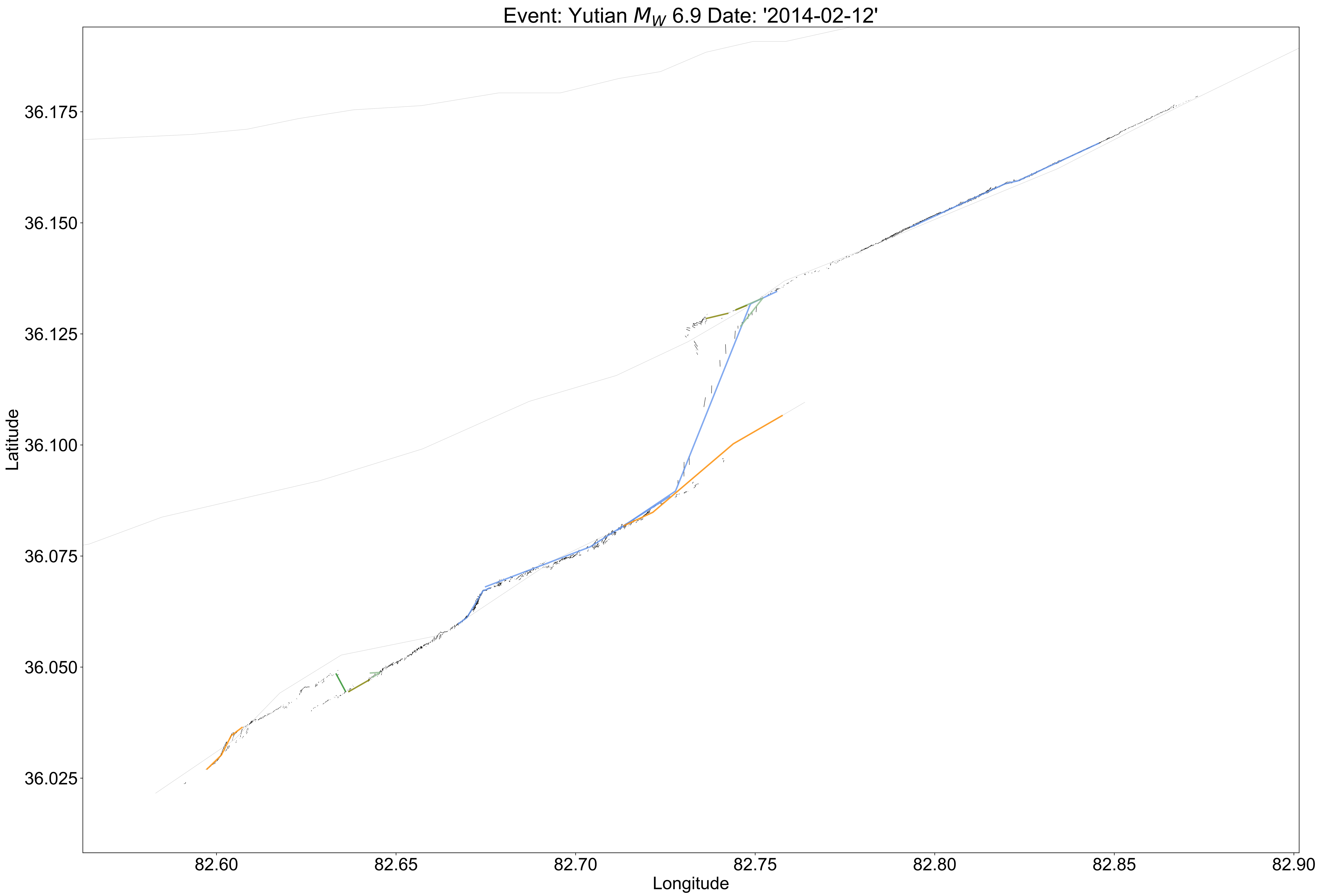
Event: Yutian M_W 6.9 Date: '2014-02-12'
36.175
36.150
36.125
36.100
36.075
36.050
36.025
Latitude
82.60
82.65
82.70
82.75
82.80
82.85
82.90
Longitude

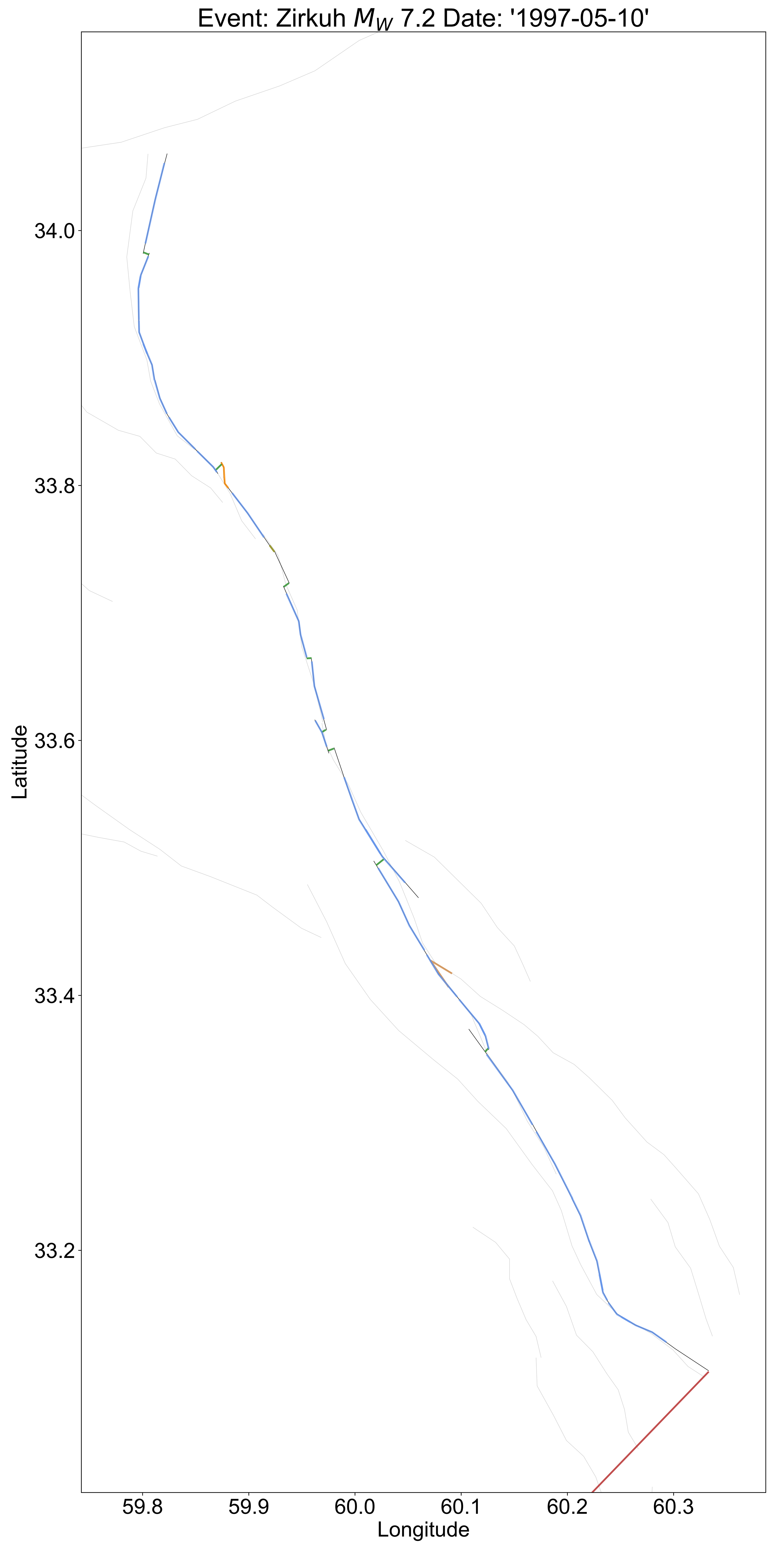
Event: Zirkuh M_W 7.2 Date: '1997-05-10'
34.0
33.8
33.6
33.4
33.2
Latitude
59.8
59.9
60.0
60.1
60.2
60.3
Longitude